# P–N and N–Mo Bond Formation Processes in the Reactions of a Pyramidal Phosphinidene-Bridged Dimolybdenum Complex with Diazoalkanes and Organic Azides

Isabel G. Albuerne, M. Angeles Alvarez, M. Esther García, Daniel García-Vivó,* Miguel A. Ruiz,* and Patricia Vega

*Departamento de Química Orgánica e Inorgánica/IUQOEM, Universidad de Oviedo, E-33071 Oviedo, Spain.*

## Abstract

The reactivity of complex [$Mo_2Cp(\mu\text{-}\kappa^1{:}\kappa^1,\eta^5\text{-}PC_5H_4)(CO)_2(\eta^6\text{-}HMes^*)(PMe_3)$] (**1**) toward different diazoalkanes and organic azides was investigated. The pyramidal phosphinidene ligand in **1** displayed a strong nucleophilicity enabling these reactions to proceed rapidly even below room temperature. Thus, **1** reacted rapidly at 253 K with different diazoalkanes $N_2CRR'$ (RR' = HH, PhPh, $HCO_2Et$) to give the corresponding *P*:*P*-bridged phosphadiazadiene derivatives as major products which, however, could not be isolated. Reaction of the latter with [$H(OEt_2)_2$]($BAr'_4$) yielded the corresponding cationic derivatives [$Mo_2Cp\{\mu\text{-}\kappa^1_P{:}\kappa^1_P,\eta^5\text{-}P(NHNCRR')C_5H_4\}(\eta^6\text{-}HMes^*)(CO)_2(PMe_3)$]($BAr'_4$), which were isolated in ca. 70% yield. A related species [$Mo_2Cp\{\mu\text{-}\kappa^1_P{:}\kappa^1_P,\eta^5\text{-}P(NMeNCHCO_2Et)C_5H_4\}(\eta^6\text{-}HMes^*)(CO)_2(PMe_3)$]($BAr'_4$) was isolated upon reaction of the ethyl diazoacetate derivative with MeI and subsequent anion exchange with Na($BAr'_4$). Reaction of **1** with aryl azides (4-$C_6H_4Me$)$N_3$ and (4-$C_6H_4F$)$N_3$ proceeded rapidly at low temperature to give possibly the corresponding *P*:*P*-bridged phosphaimine derivatives as major products, which could be neither isolated. Protonation of these products with [$H(OEt_2)_2$]($BAr'_4$) gave the corresponding aminophosphanyl complexes [$Mo_2Cp\{\mu\text{-}\kappa^1_P{:}\kappa^1_P,\eta^5\text{-}P(NHR)C_5H_4\}(\eta^6\text{-}HMes^*)(CO)_2(PMe_3)$]($BAr'_4$), isolated in ca. 75% yield. In contrast, the result of reactions of **1** with benzyl azide was strongly dependent on temperature, including the temperature in the subsequent methylation step that gave isolable cationic derivatives. By careful choice of experimental conditions, different complexes having methylated phosphatriazadiene ligands were isolated, such as [$Mo_2Cp\{\mu\text{-}\kappa^1_P{:}\kappa^1_P,\eta^5\text{-}P(NNNMeCH_2Ph)C_5H_4\}(\eta^6\text{-}HMes^*)(CO)_2(PMe_3)$]($BAr'_4$), and the metallacyclic derivatives *syn*- and *anti*-[$Mo_2Cp\{\mu\text{-}\kappa^2_{P,N}{:}\kappa^1_P,\eta^5\text{-}P(NMeNNCH_2Ph)C_5H_4\}(\eta^6\text{-}HMes^*)(CO)(PMe_3)$]($BAr'_4$). Density functional theory calculations, along with NMR monitoring experiments, revealed that the formation of the latter products stemmed from different and kinetically favored phosphatriazadiene intermediates,

thermodynamically disfavored with respect to the denitrogenation process otherwise yielding phosphaimine derivatives.

## Introduction

Reactions of transition-metal complexes bearing terminal phosphinidene ligands (PR) towards all sort of organic molecules have been extensively investigated as synthetic routes to build unusual organophosphorus molecules on the coordination sphere of single metal atoms.[1,2] In contrast, this sort of chemistry is comparatively less developed for binuclear complexes bearing bridging phosphinidene ligands, even if a binuclear platform offers more diverse active sites, depending on the coordination mode of the PR ligand at the dimetal centre (**A** to **C** in Chart 1), and possible cooperative effects between two metal atoms, as shown by more recent work by the groups of Scheer, Carty, us, and others.[3]

**Chart 1. Coordination Modes of PR Ligands at Binuclear Complexes**

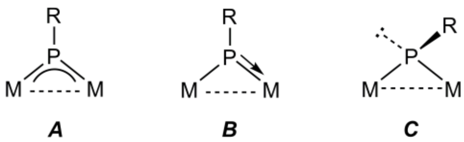


Previous work on the reactivity of binuclear phosphinidene-bridged complexes toward organic molecules is particularly scarce in the case of those containing multiple N–N bonds such as diazoalkanes and azides which, however, has revealed significant complexity. For instance, Carty *et al.* found that the trigonal phosphinidene complexes of type **A** $[Mn_2(\mu\text{-PN}^i\text{Pr}_2)(CO)_8]$ and $[Co_2(\mu\text{-PN}^i\text{Pr}_2)(CO)_4(\mu\text{-Ph}_2PCH_2PPh_2)]$ reacted with diazoalkanes or azides to yield derivatives with either bridging phosphadiazadiene, phosphaalkene or phosphaimine ligands, depending on the metal and the particular reagent,[4] with the latter two ligands following from spontaneous denitrogenation processes (Scheme 1).

**Scheme 1. Azide and Diazoalkane Derivatives of PR-Complexes of type A**[a]

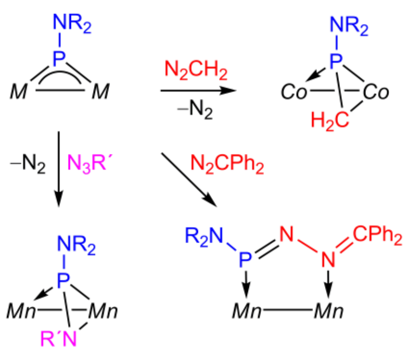


[a] *Mn–Mn*= $Mn_2(CO)_8$; *Co–Co* = $Co_2(CO)_4(\mu\text{-PPh}_2CH_2PPh_2)$; R = $^i$Pr; R'= Ph, $SiMe_3$, $SnPh_3$.

Scheer et al. also found that reactions of $[W_2(\mu\text{-PCp*})(CO)_{10}]$ with diazoalkanes can lead to phosphadiazadiene- or phosphaalkene-bridged derivatives, depending on the particular reagent used ($N_2CPh_2$ vs. $N_2CH_2$), although additional products were observed in the reaction with diazomethane.[5] In contrast, reaction of this ditungsten complex with azides $N_3R$ (R = Hex, Cy) proceeded selectively without denitrogention to yield triazaphosphete-bridged complexes (Scheme 2), which model the intermediate species proposed for the Staudinger reaction.[6]

**Scheme 2. Azide Derivatives of PR-Complexes of type A*a***

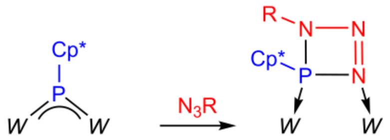


[a] *W* = W(CO)$_5$; Cp* = $C_5Me_5$; R = Hex, Cy

On the other hand, we found that spontaneous denitrogenation also dominated reactions of the trigonal phosphinidene complex of type **B** [$Mo_2Cp(\mu\text{-}\kappa^1\text{:}\kappa^1,\eta^5\text{-}PC_5H_4)(CO)_2(\eta^6\text{-HMes*})$] (Cp = $\eta^5$-$C_5H_5$; Mes* = 2,4,6-$C_6H_2{}^tBu_3$) with different diazoalkanes, which yielded in all cases the corresponding $\kappa^1$:$\eta^2$ phosphaalkene-bridged derivatives, although an unprecedented and reversible H-shift resulting in the formation of a MoNNCP metallacycle was detected for diazomethane on the way to the final phosphaethene product (Scheme 3).[7] We note that the electron contribution of the phosphaalkene ligand to the dimetal site in the dimolybdenum complexes is distinctly distributed than in the dicobalt complex mentioned above (Scheme 1), as a result of the different electronic requirements of the metal centers in each case.

**Scheme 3. Diazoalkane Derivatives of PR-Complexes of type B*a***

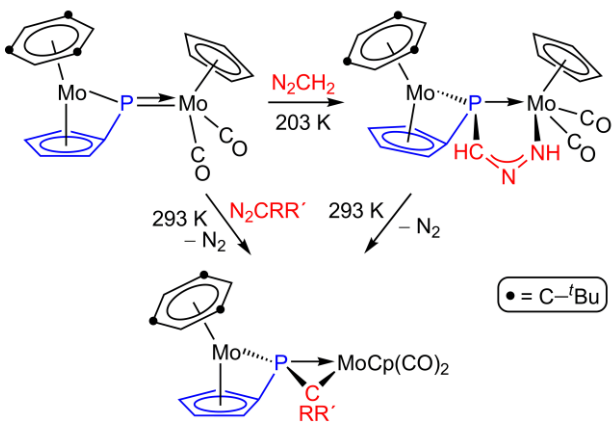


[a] RR’ = HH, PhPh, HSiMe$_3$.

In contrast, we observed no denitrogenation in the room temperature reactions of pyramidal phosphinidene complexes (type **C**) [$Fe_2Cp_2(\mu\text{-PR})(\mu\text{-CO})(CO)_2$] (R = Cy, Ph, Mes*) with benzyl azide and different diazoalkanes, which instead yielded isolable $\kappa^1{}_P$:$\kappa^1{}_P$-phosphatriazadiene- and phosphadiazadiene-bridged derivatives, respectively (Scheme 4).[8-10] Subsequent denitrogenation could be induced thermally in the first case, to give the corresponding $\kappa^1_P:\kappa^1_P$-phosphaimine-bridged complex.[9] Interestingly, reorganization of the diazoalkane derivatives could only be induced upon photochemical decarbonylation of the products first formed, which in most cases involved no denitrogenation, but gave complexes with phosphadiazadiene ligands displaying novel *P*,*C*- and *P*,*N*-bound coordination modes, as the ones shown in Scheme 4, among other unusual products.[10]

**Scheme 4. Azide and Diazoalkane Derivatives of PR-Complexes of type C*[a]***

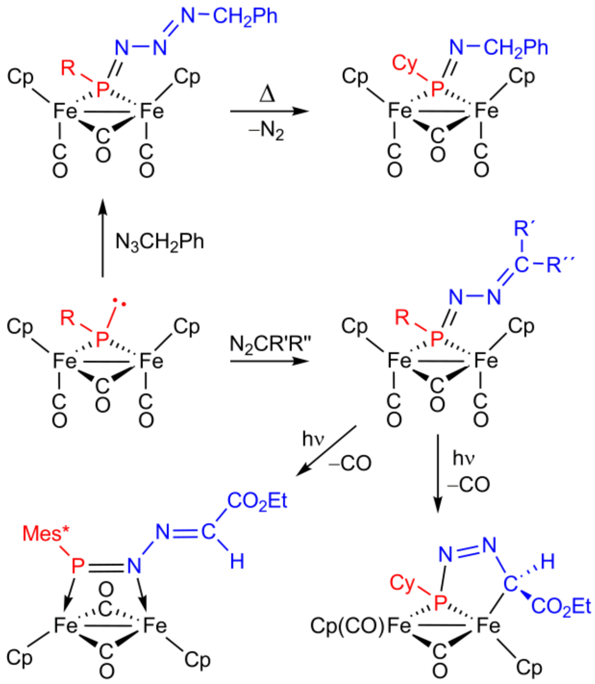


[a] R = Cy, Ph, Mes*; RR' = HH, HSiMe3, HCO2Et, PhPh.

To further explore the complex reactivity of pyramidal phosphinidene complexes towards azides and diazoalkanes, we decided to study the reactivity of the dimolybdenum complex $[Mo_2Cp(\mu\text{-}\kappa^1:\kappa^1,\eta^5\text{-}PC_5H_4)(CO)_2(\eta^6\text{-}HMes^*)(PMe_3)]$ (**1**, Chart 2) towards these unsaturated organic molecules, which is the purpose of the present work. Previous studies have revealed that **1** displays a strong nucleophilicity that enables it to react under mild conditions with different C-based electrophiles such as organic anhydrides,[11] alkyl halides,[12] and S-containing cumulenes,[13] among other electrophiles. Thus, it could be anticipated that **1** might easily react with organic azides and diazoalkanes, although the subsequent evolution of the products following the initial P–N bond formation step would be harder to predict, particularly because of the very different electronic environments of the Mo centers bound to the phosphinidene ligand in this molecule. As it will be seen below, complex **1** actually turned to be much more nucleophilic than the diiron complex mentioned above, and the products following the initial P–N bond formation step could only be stabilized through subsequent protonation and methylation reactions. In this way, products having methylated or protonated phosphadiazadiene, phosphaimine and unprecedented phosphatriazadiene ligands were obtained, the latter being kinetic products, according to DFT calculations.

**Chart 2**

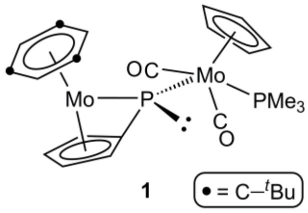


## Results and Discussion

**Reactions of Compound 1 with Diazoalkanes.** Compound **1** reacted rapidly at 253 K with different diazoalkanes $N_2CRR'$ (RR' = HH, PhPh, $HCO_2Et$) to give red solutions thought to contain the corresponding *P*:*P*-bridged phosphadiazadiene derivatives as major products, as found in the analogous reactions of $[Fe_2Cp_2(\mu\text{-PR})(\mu\text{-CO})(CO)_2]$ complexes discussed above (Scheme 4). However, all attempts to isolate these species resulted in formation of mixtures of products, from which only the corresponding protonated derivatives of type $[Mo_2Cp\{\mu\text{-}\kappa^1_P\text{:}\kappa^1_P,\eta^5\text{-P(NHNCRR')}C_5H_4\}(\eta^6\text{-HMes*})(CO)_2(PMe_3)]^+$ could be identified. These cations presumably follow from reaction of the phosphadiazadiene complex initially formed with traces of water present in the solvent. In agreement with this, the same cations could be more selectively formed upon addition of $[H(OEt_2)_2](BAr'_4)$ after reaction with the diazoalkanes (Ar' = 3,5-$C_6H_3(CF_3)_2$). This strategy enabled isolation of the corresponding tetraarylborate salts $[Mo_2Cp\{\mu\text{-}\kappa^1_P\text{:}\kappa^1_P,\eta^5\text{-P(NHNCRR')}C_5H_4\}(\eta^6\text{-HMes*})(CO)_2(PMe_3)](BAr'_4)$ (**2a-c**) in ca. 70% yield after chromatographic workup (Scheme 5). The latter suggests that initial formation of the neutral phosphadiazadiene-bridged derivatives of **1** is quite selective in all cases. However, attempts to obtain methylated derivatives analogous to complexes **2** by using MeI instead of $[H(OEt_2)_2](BAr'_4)$ were only partially successful for the $N_2CHCO_2Et$-derived species which, after workup involving anion exchange with $Na(BAr'_4)$, actually gave a 2:1 mixture of the desired complex, $[Mo_2Cp\{\mu\text{-}\kappa^1_P\text{:}\kappa^1_P,\eta^5\text{-P(NMeNCHCO_2Et)}C_5H_4\}(\eta^6\text{-HMes*})(CO)_2(PMe_3)](BAr'_4)$ (**3**), and the product of protonation **2c**. These products could not be separated from each other upon chromatographic workup, but we could obtain pure samples of **3** upon crystallization of that mixture, which enabled full structural characterization of this product (see below). Apparently, all other neutral phosphadiazadiene-bridged derivatives of **1** were too slow at reacting with MeI, and therefore decomposed or reacted with traces of water before any significant methylation could take place. Unfortunately, the use in these cases of stronger methylation reagents such as methyl triflate or $[Me_3O](BF_4)$ only yielded the protonated derivatives **2** as major products.

**Scheme 5. Diazoalkane Derivatives of 1[a]**

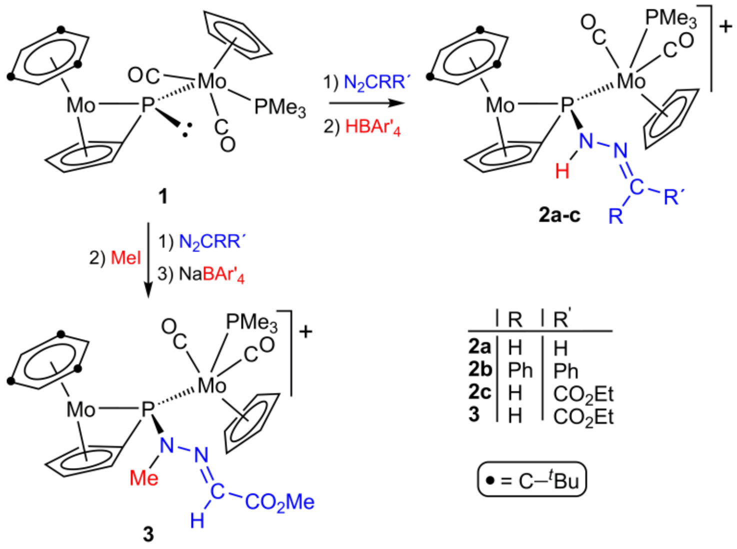


[a] Compounds **2a-c** and **3** were isolated as $BAr'_4{}^-$ salts; Ar' = 3,5-$C_6H_3(CF_3)_2$.

As noted in the Introduction, reactions of the trigonal precursor of **1** with diazoalkanes proceeded in all cases along with denitrogenation, to give the corresponding phosphaalkene derivatives (Scheme 3). In those instances, reactions seem to be initiated by diazoalkane coordination at the $Mo(CO)_2$ center, whereby the diazoalkane molecule behaves as a base, this eventually resulting in the formation of a P–C bond.[7] In the case of compound **1**, as it was also the case of diiron complexes [$Fe_2Cp_2$($\mu$-PR)($\mu$-CO)$(CO)_2$] previously investigated by us (Scheme 4), the electron-precise and nucleophilic properties of its phosphinidene ligand forces the reaction to be initiated the other way, that is, with the nucleophilic attack of the P atom at the terminal N atom of the diazoalkane molecule, the latter now acting as the electrophile partner in the acid-base reaction, while precluding any P–C bond formation process, and therefore any subsequent denitrogenation. Unfortunately, the low stability and easy protonation of all phosphadiazadiene derivatives of **1** has prevented us from examining any further rearrangements of this ligand at such asymmetrical $Mo_2$ platform.

**Structures of Compounds 2b and 3**. The molecular structures of the cations of these two complexes in the crystal are very similar to each other (Figures 1 and S1, and Table 1), and their overall conformation is comparable to those of related cations of type [$Mo_2Cp\{\mu$-$\kappa^1{}_P:\kappa^1{}_P,\eta^5$-$P(X)C_5H_4\}(\eta^6$-HMes*$)(CO)_2(PMe_3)]^+$ (X = Me, SMe) derived from **1** upon reaction with suitable electrophiles.[12] Because of the peculiar orientation of the P-based lone pair in **1**, the added electrophile (here a N atom) is placed in the $Mo_2P$ plane, which is denoted by a sum of angles around P close to 360$^o$ (359.7 and 359.8$^o$ for **2b** and **3**, respectively). The $C^1$ atom of the $C_5H_4$ ring occupies the fourth coordination position around the P atom, and defines an angle of ca. 60$^o$ with respect to the $Mo_2PN$ plane, thus completing a distorted trigonal bipyramidal (TBP) environment around the P atom, as found in the mentioned derivatives of **1**. This local geometry around phosphorus has been also found in different derivatives of the trigonal phosphinidene complex [$Mo_2Cp\{\mu-\kappa^1:\kappa^1,\eta^5-PC_5H_4\}(\eta^6$-HMes*)$(CO)_2$] with carbene,[7] chalcogens,[14] alkynes,[15] and metal carbonyl fragments[16] added at the Mo−P multiple bond of this substrate, although in these cases steric effects seem to play a significant role too. We further note that the P atom in compounds **2b** and **3** bridges the Mo atoms in a symmetrical way (Mo−P lengths ca. 2.50 Å) and that the $C_5$ rings are placed on the same side of the $Mo_2PN$ plane (*syn* conformation).

As for the built-in PNNC chain, we note that these four atoms are placed almost in the same plane, with a zig-zag conformation, thus minimizing steric repulsions while enabling some delocalization of $\pi$-bonding interactions. Indeed, P−N (1.709(3)/1.760(4) Å) and N−N distances (1.374(4)/1.351(6) Å) in this chain have values intermediate between the corresponding reference figures for single and double bonds (P−N = 1.78; P=N = 1.57; N−N = 1.42, N=N = 1.25 Å).[17,18] These values, in turn, are somewhat longer and shorter, respectively, than those determined previously for the diiron complex [$Fe_2Cp_2\{\mu-\kappa^1_P:\kappa^1_P$-CyPNHNCH$_2$)($\mu$-CO)$(CO)_2$]($BF_4$) (1.669(2) and 1.3882(2) Å).[10] Besides this, the N−C lengths of ca. 1.29 Å in our dimolybdenum complexes are very close to the reference value of 1.27 Å for a N=C($sp^2$) double bond, and the added proton/methyl is located at the P-bound N atom, which displays no significant pyramidalization, as found in the mentioned diiron complex. In all, the above structural parameters justify the description of the P-donor bridging ligands in compounds **2b** and **3** as aminophosphanyl ligands, with the lone electron pair at the N1 atom being involved in a moderate $\pi$ bonding interaction with both the P1 and N2 atoms.

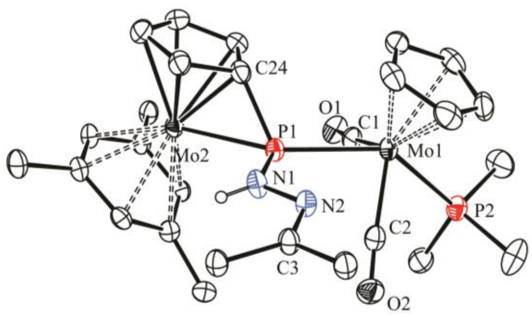


**Figure 1**. ORTEP diagram (30% probability) of the cation in compound **2b**, with $^t$Bu and Ph groups (except their $C^1$ atoms) and most H atoms omitted for clarity.

**Table 1.** Selected Bond Lengths (Å) and Angles (º) for Compounds **2b** and **3**

| | **2b** | **3** |
|---|---|---|
| Mo1–P1 | 2.4923(8) | 2.495(1) |
| Mo2–P1 | 2.5022(8) | 2.524(1) |
| Mo1–P2 | 2.4689(9) | 2.470(1) |
| Mo1–C1 | 1.980(4) | 1.984(5) |
| Mo1–C2 | 1.983(4) | 1.968(6) |
| P1–C24/16 | 1.791(3) | 1.792(5) |
| P1–N1 | 1.709(3) | 1.760(4) |
| N1–N2 | 1.374(4) | 1.351(6) |
| N1–H/C3 | 0.79(8) | 1.462(6) |
| N2–C3/4 | 1.295(4) | 1.284(6) |
| Mo1–P1–Mo2 | 139.71(4) | 136.35(4) |
| Mo1–P1–N1 | 112.8(1) | 110.2(1) |
| Mo2–P1–N1 | 107.2(1) | 113.2(1) |
| Mo2–P1–C24/16 | 58.8(1) | 58.2(2) |
| P1–Mo1–P2 | 137.60(3) | 137.05(4) |
| C1–Mo1–C2 | 107.0(1) | 105.4(2) |
| C1–Mo1–P1 | 80.4(1) | 77.6(1) |
| C1–Mo1–P2 | 77.6(1) | 81.3(1) |

**Structure of Compounds 2 and 3 in Solution**. Spectroscopic data in solution for compounds **2a-c** and **3** (Table 2, Experimental Section, and SI) are comparable to each other, and are consistent with retention in solution of the crystal structures discussed above. In particular, all four compounds display two C–O stretching bands with relative intensities (medium and strong, in order of decreasing frequency) characteristic of transoid $M(CO)_2$ oscillators,[19] as found in the crystal for **2b** and **3** (C–Mo–C angles ca. 106º). This is also reflected in the observation, for the corresponding $^{13}C$ NMR resonances, of a relatively high coupling of ca. 28 Hz with both P atoms of the molecule.[20] The newly formed phosphanyl ligands display resonances in the range 104.6-144.9 ppm, close to the chemical shift of the parent phosphinidene complex ($\delta_P$ 122.0 ppm),[11] and their couplings to the $PMe_3$ ligands are large (ca. 30 Hz). The latter seems to be a diagnostic signature for all derivatives of **1** displaying a *syn* conformation of their $C_5$ rings.[12] Finally we note that, in the case of compounds **2**, the added proton gives rise to a moderately deshielded ($\delta_H$ 5.9-6.5 ppm) and strongly P-coupled $^1H$ NMR resonance ($^2J_{PH}$ = 16-20 Hz), which is replaced by a methyl resonance at 3.37 ppm ($^3J_{PH}$ = 5 Hz) in the case of **3**. Other spectroscopic features of these complexes are as expected and deserve no detailed comments.

**Table 2.** Selected IR and $^{31}P\{^1H\}$ NMR Data for New Isolated Compounds.[a]

| Compound | $\nu$(CO) | $\delta(PC_5H_4)$ | $\delta(PMe_3)$ | $J_{PP}$ |
|---|---|---|---|---|
| $[Mo_2Cp(\mu-\kappa^1_P:\kappa^1_P,\eta^5-PC_5H_4)(\eta^6-HMes^*)(CO)_2(PMe_3)]$ (**1**)[b] | 1910 (m), 1842 (vs) | 122.0 | 27.3 | 26 |
| $[Mo_2Cp\{\mu-\kappa^1_P:\kappa^1_P,\eta^5-P(NHNCH_2)C_5H_4\}(\eta^6-HMes^*)(CO)_2(PMe_3)](BAr'_4)$ (**2a**) | 1969 (m), 1889 (vs) | 104.6[c] | 18.5[c] | 30 |
| $[Mo_2Cp\{\mu-\kappa^1_P:\kappa^1_P,\eta^5-P(NHNCPh_2)C_5H_4\}(\eta^6-HMes^*)(CO)_2(PMe_3)](BAr'_4)$ (**2b**) | 1968 (m), 1889 (vs) | 105.6 | 18.4 | 30 |
| $[Mo_2Cp\{\mu-\kappa^1_P:\kappa^1_P,\eta^5-P(NHNCHCO_2Et)C_5H_4\}(\eta^6-HMes^*)(CO)_2(PMe_3)](BAr'_4)$ (**2c**) | 1970 (m), 1890 (vs) | 113.5 | 17.9 | 31 |
| $[Mo_2Cp\{\mu-\kappa^1_P:\kappa^1_P,\eta^5-P(NMeNCHCO_2Et)C_5H_4\}(\eta^6-HMes^*)(CO)_2(PMe_3)](BAr'_4)$ (**3**) | 1966 (m), 1887 (vs) | 144.9 | 18.6 | 29 |
| $[Mo_2Cp\{\mu-\kappa^1_P:\kappa^1_P,\eta^5-P(NH(4-C_6H_4Me))C_5H_4\}(\eta^6-HMes^*)(CO)_2(PMe_3)](BAr'_4)$ (**4d**) | 1963 (m), 1888 (vs) | 87.2[c] | 19.6[c] | 22 |
| $[Mo_2Cp\{\mu-\kappa^1_P:\kappa^1_P,\eta^5-P(NH(4-C_6H_4F))C_5H_4\}(\eta^6-HMes^*)(CO)_2(PMe_3)](BAr'_4)$ (**4e**) | 1964 (m), 1889 (vs) | 88.7 | 19.5 | 22 |
| $[Mo_2Cp\{\mu-\kappa^1_P:\kappa^1_P,\eta^5-P(NHCH_2Ph)C_5H_4\}(\eta^6-HMes^*)(CO)_2(PMe_3)](BAr'_4)$ (**4f**) | 1965 (m), 1888 (vs) | 101.1(br) | 18.8 | 30 |
| $[Mo_2Cp\{\mu-\kappa^1_P:\kappa^1_P,\eta^5-P(NMe(4-C_6H_4F))C_5H_4\}(\eta^6-HMes^*)(CO)_2(PMe_3)](BAr'_4)$ (**5**) | 1960 (m), 1883 (vs) | 105.8 | 19.4 | 25 |
| $[Mo_2Cp\{\mu-\kappa^1_P:\kappa^1_P,\eta^5-P(NNNMeCH_2Ph)C_5H_4\}(\eta^6-HMes^*)(CO)_2(PMe_3)](BAr'_4)$ (**6**) | 1963 (m), 1885 (vs) | 124.4 (br)[c] | 20.2[c] | 24 |
| *syn*-$[Mo_2Cp\{\mu-\kappa^2_{P,N}:\kappa^1_P,\eta^5-P(NMeNNCH_2Ph)C_5H_4\}(\eta^6-HMes^*)(CO)(PMe_3)](BAr'_4)$ (***syn*-7**) | 1860 (vs) | 208.2 | 7.2 | 17 |
| *anti*-$[Mo_2Cp\{\mu-\kappa^2_{P,N}:\kappa^1_P,\eta^5-P(NMeNNCH_2Ph)C_5H_4\}(\eta^6-HMes^*)(CO)(PMe_3)](BAr'_4)$ (***anti*-7**) | 1850 (vs) | 227.7 | 13.3 | 35 |

[a] IR data recorded in dichloromethane solution, with C–O stretching bands [$\nu$(CO)] in $cm^{-1}$; NMR data recorded in $CD_2Cl_2$ solution at 121.48 MHz and 293 K, with chemical shifts ($\delta$) in ppm relative to external 85% aqueous $H_3PO_4$, and P-P couplings ($J_{PP}$) in hertz. [b] Data taken from reference 11; IR data in toluene solution; NMR data in $C_6D_6$ solution. [c] Data recorded at 233 K.

**Reactions of Compound 1 with Organic Azides.** As found in its reactions with diazoalkanes, compound **1** reacted rapidly with different organic azides, but again the products formed initially were very unstable, and it was only upon subsequent protonation or methylation that stable species could be obtained and isolated. Moreover, the result of these reactions was strongly dependent on the particular azide used, also on experimental conditions (Schemes 6 and 7).

Reaction of **1** with aryl azides $N_3(4-C_6H_4Me)$ and $N_3(4-C_6H_4F)$ proceeded rapidly at low temperature to give brown-greenish suspensions thought to contain the corresponding *P*:*P*-bridged phosphaimine derivatives as major products. These would be comparable to those formed, after thermally-induced denitrogenation, in the analogous reactions of complex $[Fe_2Cp_2(\mu-PCy)(\mu-CO)(CO)_2]$ mentioned above (Scheme 4). Such a hypothesis is based on the nature of their isolable derivatives, and is further supported by results of DFT calculations to be discussed below. In any case, upon protonation of these suspensions with $[H(OEt_2)_2](BAr'_4)$, green solutions of the corresponding aminophosphanyl-bridged derivatives $[Mo_2Cp\{\mu-\kappa^1_P:\kappa^1_P,\eta^5-P(NHR)C_5H_4\}(\eta^6-HMes^*)(CO)_2(PMe_3)](BAr'_4)$ (R = $4-C_6H_4Me$ (**4d**), $4-C_6H_4F$ (**4e**)) were formed as major products, which could be isolated in ca. 75% yield after chromatographic workup. The neutral intermediate following reaction of **1** with $N_3(4-C_6H_4F)$ was nucleophilic enough to react with MeI before major decomposition or reaction with traces of water present in the solvent could take place. Even so, after anion exchange with Na(BAr'$_4$), a 2:1 mixture was obtained of the methylated product [Mo$_2$Cp{$\mu$-$\kappa^1_{\mathrm{P}}$:$\kappa^1_{\mathrm{P}}$,$\eta^5$-P(NMe(4-C$_6$H$_4$F))C$_5$H$_4$}($\eta^6$-HMes*)(CO)$_2$(PMe$_3$)](BAr'$_4$) (**5**) and the corresponding product of protonation **4e**, from which it could not be separated upon chromatographic workup. Unfortunately, attempts to grow crystals of **5** suitable for a diffraction study were in this case unsuccessful. Yet, spectroscopic data in solution for this complex support a structure comparable to those of the protonation products of type **4**, as discussed later on.

**Scheme 6. Aryl Azide Derivatives of 1**[a]

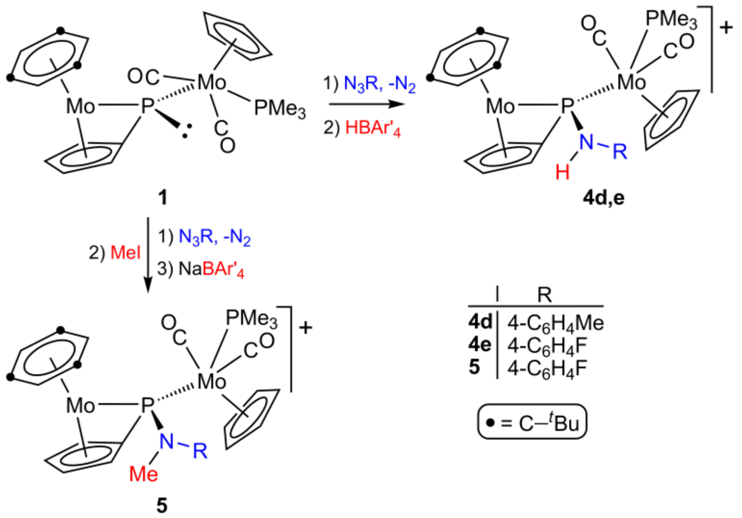


[a] Compounds **4d,e** and **5** were isolated as BAr'$_4^-$ salts; Ar' = 3,5-C$_6$H$_3$(CF$_3$)$_2$.

In contrast with the above results, the reactions of **1** with benzyl azide were strongly dependent on the temperature at which they were carried out. Besides this, temperature was also critical in the subsequent methylation steps that gave isolable cationic derivatives (Scheme 7). Thus, when reaction of **1** with benzyl azide was performed at 223 K, a green solution was rapidly formed, thought to contain the corresponding *P*:*P*-bridged phosphatriazadiene derivative. Reaction of this solution with MeI at the same temperature and subsequent anion exchange at room temperature using Na(BAr'$_4$) gave the phosphanyl complex [Mo$_2$Cp{$\mu$-$\kappa^1_{\mathrm{P}}$:$\kappa^1_{\mathrm{P}}$,$\eta^5$-P(NNNMeCH$_2$Ph)C$_5$H$_4$}($\eta^6$-HMes*)(CO)$_2$(PMe$_3$)](BAr'$_4$) (**6**) in good yield, a product derived from methylation at the remote N atom of the phosphatriazadiene ligand. However, when reaction of **1** with benzyl azide was performed at 253 K, a red solution was rapidly formed instead. Subsequent reaction with MeI at the same temperature gave, after anion exchange at room temperature using Na(BAr'$_4$), the phosphatriazametallacyclic derivative *syn*-[Mo$_2$Cp{$\mu$-$\kappa^2_{\mathrm{P,N}}$:$\kappa^1_{\mathrm{P}}$,$\eta^5$-P(NMeNNCH$_2$Ph)C$_5$H$_4$}($\eta^6$-HMes*)(CO)(PMe$_3$)](BAr'$_4$) (***syn*-7**), which was isolated in ca. 70% after chromatographic workup and displays a Me group at the P-bound nitrogen atom. Yet, if the methylation step was performed at room temperature, then an isomer of the above metallacyclic product (***anti*-7**) was isolated in ca. 80% after similar workup, with the $C_5$ rings of the molecule being now arranged on different sides of the average $MoPN_3$ metallacycle plane.

**Scheme 7. Benzyl Azide Derivatives of 1[a]**

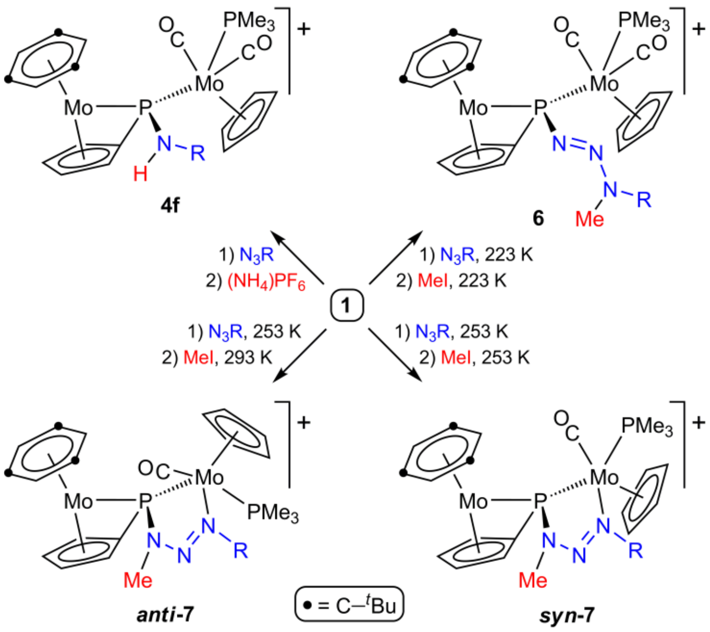


[a] All derivatives of **1** were isolated as $BAr'_4{}^-$ salts; Ar' = 3,5-$C_6H_3(CF_3)_2$; R = $CH_2Ph$.

$^{31}$P NMR monitoring experiments revealed that the major neutral species present at each of the above temperatures before the methylation step were indeed different from each other. Thus, upon reaction of **1** with $N_3CH_2Ph$ in toluene-$d_8$ at 223 K, the $^{31}$P NMR spectrum displayed dominant resonances at ca. 415.4 and 26.5 ppm, with a mutual PP coupling of 42 Hz, which we assign to the phosphatriazadiene precursor of **6**. Upon warming the NMR tube up to 253 K, these resonances progressively faded out and were replaced by two new couples of doublets at 219.3/12.6 ppm (major, $J_{PP}$ = 18 Hz) and 226.2/16.6 ppm (minor, $J_{PP}$ = 22 Hz), which we identify as arising from the neutral precursors of isomers ***syn*-7** and ***anti*-7**, respectively. Indeed, upon further warming of this solution up to room temperature, the first couple of resonances vanished progressively at the expense of the second couple. Addition of MeI to the NMR tube at this final stage gave ***anti*-7** as the major product, in agreement with results of the reactions carried out on the preparative scale. Surprisingly, protonation of any of the above neutral intermediates triggered their denitrogenation, to give the same cationic complex in all cases as major product, along with other uncharacterized species. This complex could be conveniently isolated as the corresponding tetraarylborate salt $[Mo_2Cp\{\mu\text{-}\kappa^1_P:\kappa^1_P,\eta^5\text{-}P(NHCH_2Ph)C_5H_4\}(\eta^6\text{-}HMes^*)(CO)_2(PMe_3)](BAr'_4)$ (**4f**) in moderate yield (see the Experimental Section). Further evidence on the nature and structure of the neutral precursors of compounds **4f**, **6** and **7** was obtained through DFT calculations to be discussed later on.

**Structural Characterization of Compounds 4 and 5.** These compounds displayed C−O stretches and $^{31}$P NMR parameters comparable to those of complexes **2** and **3** (Table 2), this pointing to a close structural relationship, including their overall conformation (*syn* arrangement of their $C_5$ rings), with differences only arising from the nitrogenated fragment bound to the P atom in each case (NRR' vs. NRN=CR'R''). Spectroscopic evidence for the denitrogenation operated in the former azide molecule on the course of formation of compounds **4** and **5** is given by the strong coupling to P of the N-bound H atom in the aminophosphanyl ligand of compounds **4d,e** ($\delta_H$ ca. 4.1 ppm; $^2J_{HP}$ = 13 Hz), which is comparable to the corresponding couplings of 16-20 Hz in compounds **2a-c** (see the Experimental Section). H−P coupling was not resolved in the NH resonance of **4f**, due to broadness, but was clearly observed for its benzyl protons ($^3J_{HP}$ = 14 Hz), as it is the case of the added methyl group in compound **5** ($\delta_H$ 3.32 ppm; $^3J_{HP}$ = 10 Hz). The latter displays a P−H coupling even higher than the one observed for compound **3** ($\delta_H$ 3.37 ppm; $^3J_{HP}$ = 5 Hz). As additional comparison, we note that the NH resonance of the crystallographically characterized diiron complex [$Fe_2Cp_2${$\mu$-$\kappa^1_P$:$\kappa^1_P$-P($NHCH_2Ph$)Cy}($\mu$-CO)$(CO)_2$]$BF_4$ appeared at 4.40 ppm, and displayed a P−H coupling of 5 Hz.[9]

**Structure of Compound 6.** The overall structure of the cation of compound **6** in the crystal (Figure 2 and Table 3) is comparable to those found for compounds **2b** and **3**, except for the internal parameters in the nitrogenated chain attached to the P atom. As found in the mentioned complexes, the P atom is bound to both Mo atoms in a rather symmetrical way (Mo1−P1 = 2.550(1), Mo2−P1 = 2.509(1) Å), and the P-bound N atom is placed in the $Mo_2P$ plane (sum of angles around P ca. 360°), with the C atom of the $C_5H_4$ ring then completing a distorted TBP environment around phosphorus. Both $C_5$ rings of the cation are placed on the same side of the $Mo_2PN$ plane (*syn* conformation), as found for the mentioned complexes, and the MoCp fragment also retains the transoid local geometry of the parent complex, with P−Mo−P and OC−Mo−CO angles of 138.49(5) and 107.2(3)°, respectively.

As for the geometry of the methylated triazaphosphadiene ligand in **6**, we first note that all atoms in the P−N−N−N−C chain (angles ca. 113-123°) are placed almost in the same plane, thus enabling $\pi$ bonding interactions. Although no metal complexes bearing triazaphosphadiene or alkylated triazaphosphadiene ligands seem to have been structurally characterized to date, we note that similar arrangements have been found in phosphine-azide adducts $R_3P$−$N_3R'$,[21] which are well known intermediates in the preparation of iminophosphines $R_3P$=NR', in a process known as the Staudinger reaction.[22] In the above adducts, typical interatomic distances in the P−N−N−N chain are ca. 1.65, 1.33 and 1.28 Å,[23] indicative of bond orders intermediate between 1 and 2,[17,18] which can be compared to the figures of 1.736(5), 1.262(8), and 1.312(8) Å for the corresponding bonds in **6**. Thus, it seems that methylation at the remote NR atom of a coordinated phosphatriazadiene ligand increases the double-bond character of the central N–N bond of the chain, which now approaches the reference value of ca. 1.25 Å for a N=N bond. Yet, the external P–N and N–N bonds in **6** are still shorter than the respective reference single-bond values of 1.78 and 1.42 Å,[17] which points to the presence of some *π*-bonding delocalization originated in the lone electron pair of the terminal NMe$CH_2$Ph group of the ligand. This effect can be represented through the canonical forms depicted in Chart 3.

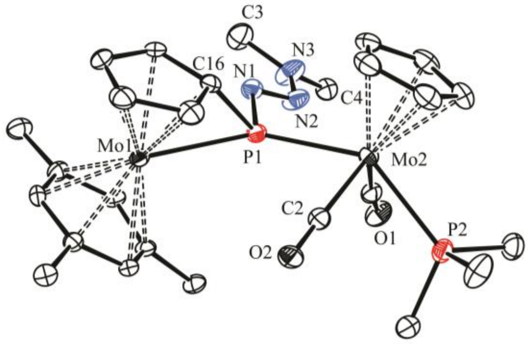


**Figure 2**. ORTEP diagram (30% probability) of the cation in compound **6** with $^t$Bu and $CH_2$Ph groups (except their C[1] atoms) and H atoms omitted for clarity. Atom C4 belongs to the benzyl group.

**Table 3.** Selected Bond Lengths (Å) and Angles (º) for Compound **6**

| | | | |
|---|---|---|---|
| Mo1–P1 | 2.550(1) | Mo1–P1–Mo2 | 140.01(6) |
| Mo2–P1 | 2.509(1) | Mo1–P1–N1 | 104.7(2) |
| Mo2–P2 | 2.472(2) | Mo2–P1–N1 | 115.3(2) |
| Mo2–C1 | 2.008(7) | Mo1–P1–C16 | 57.7(2) |
| Mo2–C2 | 1.970(6) | P1–Mo2–P2 | 138.49(5) |
| P1–C16 | 1.785(6) | C1–Mo2–C2 | 107.2(3) |
| P1–N1 | 1.736(5) | C1–Mo2–P1 | 80.9(2) |
| N1–N2 | 1.262(8) | C1–Mo2–P2 | 75.0(2) |
| N2–N3 | 1.312(8) | P1–N1–N2 | 113.4(4) |
| N3–C3 | 1.44(1) | N1–N2–N3 | 114.5(5) |
| N3–C4 | 1.44(2) | N2–N3–C3 | 122.9(6) |
| | | N2–N3–C4 | 120.9(7) |

## Chart 3

Spectroscopic data for compound **6** in solution (Table 2, Experimental Section, and SI) are consistent with the structure found in the solid state, and support its retention in solution. In particular, the observation of a relatively high P-P coupling of 24 Hz suggests the predominance in solution of the *syn* conformation found in the crystal, as also found for compounds **2** to **5**. The methyl group bound to the remote N atom displays no measurable coupling to phosphorus, as expected for a connection through five bonds (cf. 5 to 10 Hz for the three-bond P-H coupling in compounds **3** and **5**). Other spectroscopic data for **6** are comparable to those measured for compounds **2** to **5** and need not to be discussed.

**Structure of Compounds 7.** In the crystal, the cation of compound ***anti*-7** (Figure 3 and Table 4) displays a phosphatriazadiene ligand methylated at the P-bound N atom, which binds the metallocene Mo fragment through its P atom, while binding a MoCp(CO)($PMe_3$) fragment through both the P atom and the remote N atom, thus defining a somewhat twisted $MoPN_3$ metallacycle. To our knowledge, no metal complex with a RPNR'NNR'' ligand has been previously reported nor structurally characterized, although a cyclic derivative of such a ligand has been recently identified in complex [{W$(CO)_5$}$_2${P(Cp*)-N(N=$CH_2$)-N=N-$CH_2$}].[5] The local geometry around the P atom in this ligand is of the distorted TBP type found in compounds **2b**, **3** and **6**, with the N1 atom placed almost in the $Mo_2P$ plane (sum of angles around P ca. 358.5°), while the arrangement of ligands around the MoCp fragment is also similar to the one found in the mentioned compounds, with P atoms *trans* to each other (P1−Mo1−P2 = 129.35(5)°), and the unique carbonyl ligand *trans* to the coordinated N atom (C1−Mo1−N3 = 109.7(2)°). However, the relative arrangement of both metal fragments in ***anti*-7** is different from the one found in the mentioned compounds, as now the $C_5$ rings of the molecule are positioned on opposite sides of the $Mo_2PN$ average plane (*anti* conformation).

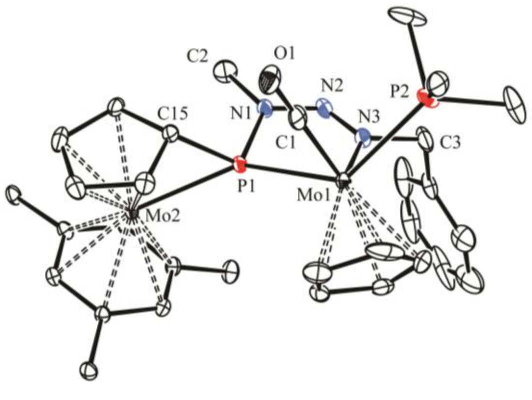


**Figure 3**. ORTEP diagram (30% probability) of the cation in compound ***anti*-7**, with $^t$Bu groups (except their $C^1$ atoms) and H atoms omitted for clarity.

**Table 4.** Selected Bond Lengths (Å) and Angles (º) for Compound ***anti*-7**

| | | | |
|---|---|---|---|
| Mo1–P1 | 2.444(1) | Mo1–P1–Mo2 | 143.44(5) |
| Mo2–P1 | 2.505(1) | Mo1–P1–N1 | 98.6(1) |
| Mo1–P2 | 2.480(1) | Mo2–P1–N1 | 116.6(1) |
| Mo1–C1 | 1.924(6) | Mo2–P1–C15 | 59.1(2) |
| Mo1–N3 | 2.186(5) | P1–Mo1–P2 | 129.35(5) |
| P1–C15 | 1.782(5) | C1–Mo1–N3 | 109.7(2) |
| P1–N1 | 1.748(4) | C1–Mo1–P1 | 75.4(2) |
| N1–N2 | 1.336(6) | C1–Mo1–P2 | 73.4(1) |
| N2–N3 | 1.290(6) | P1–N1–N2 | 119.2(3) |
| N3–C3 | 1.491(6) | N1–N2–N3 | 114.4(4) |
| N1–C2 | 1.472(7) | N2–N3–Mo1 | 127.1(3) |
| | | N2–N3–C3 | 108.5(5) |

As for the interatomic distances within the $MoPN_3$ metallacycle, we note that the Mo1–P1 distance is somewhat shorter than the Mo2–P1 one (2.444(1) vs. 2.505(1) Å), possibly due to geometrical restrictions imposed by the ring. Besides this, the Mo1–N3 distance of 2.186(5) Å is comparable to the corresponding distances measured in amidinate complexes of type [Mo($\eta^5$-L)($\kappa^2$-NRCR´NR)$(CO)_2$] (L = Cp or related ligand), which are found in the range 2.15-2.19 Å.[24] Surprisingly, the P–N distance in ***anti*-7** is comparable to the one measured in **6** (1.748(4) vs. 1.736(5) Å), in spite of the methylation operated at this N site in the metallacyclic complex. The N–N distances, however, have been modified significantly, with the central N–N bond of the former phosphatriazadiene ligand being now the longer one (N1–N2 = 1.336(6), N2–N3 = 1.290(6) Å). Yet, these distances have values intermediate between the reference figures for single and double N–N bonds (1.42/1.25 Å), which is indicative of substantial delocalization of the $\pi$ bonding interactions between N atoms, an effect that can be represented through the canonical forms depicted in Chart 4.

**Chart 4**

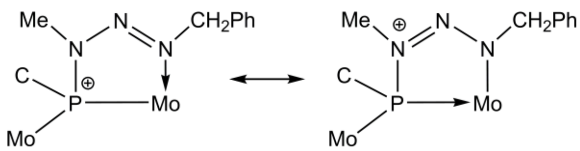


Spectroscopic data for compound ***anti*-7** in solution (Table 2, Experimental Section, and SI) are consistent with the structure found in the solid state, and deserve only a few comments. The most noticeable spectroscopic feature concerns the $^{31}P$ NMR resonance for the bridging P atom ($\delta_P$ 227.7 ppm, $J_{PP}$ = 35 Hz), which displays a chemical shift some 100 ppm above the one for **6** or any of compounds **2** to **5**, while its coupling to the $PMe_3$ ligand is significantly higher too. None of these differences can be attributed to the different bond angles involving the phosphanyl-like bridging P atom in ***anti*-7**, which are similar to the corresponding angles in all other complexes.[25,20] We rather attribute the strong deshielding of this P atom to the combined effect of substitution of a carbonyl ligand with a strong N donor at the MoCp fragment, along with the formation of a five-membered ring.[26] On the other hand, the strong P-P coupling observed for ***anti*-7** might be related to the relatively short Mo–P distance within this ring, already mentioned. We finally note that the retention in solution of the *anti* conformation of the $C_5$ rings found in the solid-state structure was confirmed through a standard NOESY experiment, which revealed positive NOE effects between Cp and $^t$Bu protons. These NOE effects were absent in the corresponding NOESY spectrum of ***syn*-7**, which is thus identified as an isomer having $C_5$ rings placed on the same side of the average metallacycle plane, whereby the Cp ligand is positioned far away the $C_6H_3{}^tBu_3$ group. Other spectroscopic properties for ***syn*-7** (Table 2, Experimental Section, and SI) are comparable to those of its *anti* isomer and deserve no detailed comment. We note, however, that P-P coupling in the *cis* isomer (17 Hz) is almost halved when compared to the one in the *anti* isomer (35 Hz), an observation for which we cannot give a satisfactory explanation at present.

**Pathways in the Reactions of 1 with Organic Azides.** In the preceding sections we have provided spectroscopic evidence to support that each of the benzyl azide derivatives **6**, ***syn*-7** and ***anti*-7** arise from different neutral intermediates, presumably displaying bridging phosphatriazadiene ligands. To give further support to the above proposal, and also to gain some insight into the distinct behavior of benzyl azide in this context, when compared to aryl azides, we carried out DFT calculations (see the Experimental Section and SI)[27] on the structures of the neutral intermediates (**A** to **E**, Scheme 8) most likely involved in these reactions. The structures of complexes **6** and ***anti*-7** were used as starting models for the different intermediates under study, and the optimized structures for benzyl azide derivatives (**A1** to **E1**) are shown in Figure 4 (see Figure S2 for other derivatives), while Table 5 collects the relative energies for all these neutral species.

Reactions between the phosphinidene complex **1** and organic azides would be initiated by the nucleophilic attack of the phosphinidene P atom to the terminal nitrogen of the organic reagent, to form *P*:*P*-bridged phosphatriazadiene complexes **A**, as observed in related reactions of diiron complexes $[Fe_2Cp_2(\mu\text{-PR})(\mu\text{-CO})(CO)_2]$ (R = Cy, Ph).[8,9] Intermediate **A1** presumably would be the species responsible for the $^{31}$P NMR resonance at 415.4 ppm observed at 223 K in the monitoring experiments of the benzyl azide reaction discussed above (see Fig. S35). This intermediate would display the transoid conformation of the P–N–N–N-chain that leads naturally to complex **6** upon nucleophilic attack of its remote N atom on MeI, and it has been used here as the energy reference for all other computed species.

**Scheme 8. Proposed Pathways in the Reactions of 1 with Organic Azides**

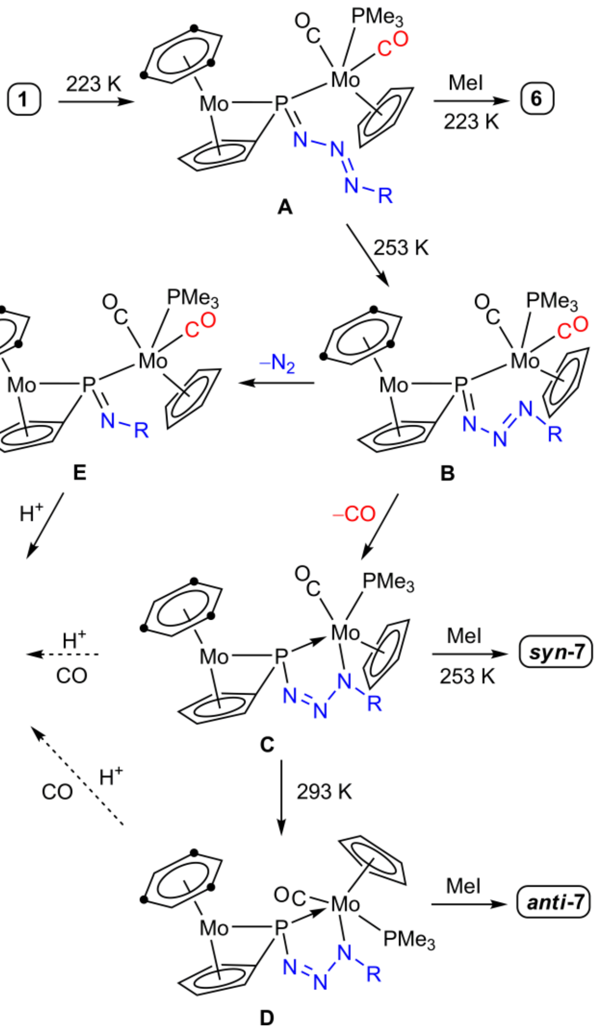


As discussed above, depending on the particular azide and experimental conditions, other products are obtained after protonation/methylation steps, they involving decarbonylation along with Mo–N bond formation (compounds **7**) or denitrogenation of the neutral intermediates initially formed (compounds **4** and **5**). This requires in any case a modification of the conformation of the P–N–N–N chain of the phosphatriazadiene ligand in intermediates **A**, from a transoid to a cisoid arrangement, so as to approach the remote N atom to either Mo or P atoms. The corresponding isomers (**B**) actually are some 15-20 kJ/mol more stable than the initial intermediates **A** in all cases.[28] This isomerization might be followed by decarbonylation, which would leave a coordination vacant at the metal site being rapidly occupied by the remote N atom of the nitrogenated ligand, then naturally yielding metallacyclic complexes of type **C**, which in turn would render, after reaction with MeI, complexes like ***syn*-7**. Intermediate **C1** presumably is the species responsible for the $^{31}$P NMR resonance at 219.3 ppm observed at 253 K in the mentioned monitoring experiments of the benzyl azide reaction (see Fig. S35). Finally, the conformational change from **C** to **D** (*syn* to *anti* rearrangement) would just require a transient N−Mo bond cleavage to allow for the necessary rotation of the MoCp(CO)($PMe_3$) fragment, this yielding a more stable isomer in all cases. We have also considered the possibility that the decarbonylation route connecting intermediates **B1** and **C1** could be initiated by the nucleophilic attack of the pendant NR group to the carbonyl ligand in intermediate **B1**, this being followed by a decarbonylation step, thus reproducing analogous reaction pathways identified in the reactions of complex [$Mo_2Cp(\mu\text{-}\kappa^1:\kappa^1,\eta^5\text{-}PC_5H_4)(CO)_2(\eta^6\text{-}HMes^*)$] with alkynes.[15,29] Such event, however, is less likely here, as the metallacyclic intermediate stemming from the corresponding N−C bond formation step was computed to be 26 kJ/mol above **B1.**

On the other hand, the denitrogenation route leading to complexes **4** and **5** would likely start from intermediates **B** too, since the latter have the right (cisoid) conformation of the P−N−N−N chain to undergo the P−NR bond formation process that gives the four-membered $PN_3$ phosphacycles eventually enabling denitrogenation, then rendering the corresponding phosphaimine complexes **E**, as proposed for reactions of phosphines with organic azides (Staudinger reaction).[21,22] This sort of transformation was actually induced thermally on the diiron complex [$Fe_2Cp_2(\mu\text{-}CyPN_3CH_2Ph)(\mu\text{-}CO)(CO)_2$], as noted in the Introduction (Scheme 4).[9] Protonation or methylation of phosphaimine intermediates **E**, of course, would naturally give the aminophosphanyl-bridged complexes **4** and **5**. We note, however, that protonation of all benzyl azide-derived intermediates (**A1** to **D1**) renders invariably the aminophosphanyl complex **4f** as major product, even if in modest yield. Since electrophilic attack at the remote NR atom in intermediates **C1** and **D1** is prevented by its coordination to the metal site, we must assume that protonation in these cases would take place at a different N atom, this being followed by a fast H-shift to the remote NR group, thus allowing for denitrogenation, although the exact sequence of events cannot be established at present.

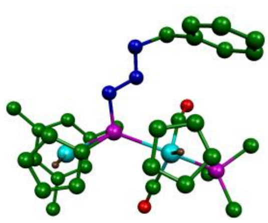

**A1**

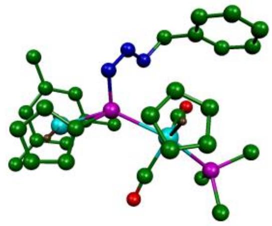

**B1**

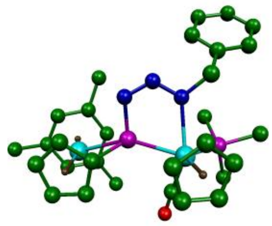

**C1**

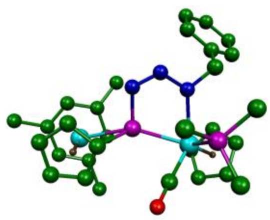

**D1**

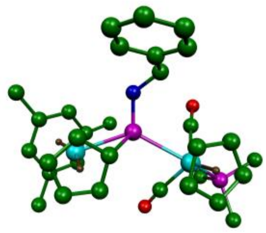

**E1**

**Figure 4**. M06L-DFT-optimized structures of likely intermediates in the reactions of **1** with benzyl azide, with $^{t}$Bu groups (except their $C^1$ atoms) and H atoms omitted.

**Table 5.** M06L-DFT- Computed Gibbs Free Energies at 298 K (kJ/mol) and Selected Bond Distances (Å) and Angles (deg.) for $N_3R$-Derivatives of Compound **1**.[a]

| Structure | R | ΔG | Mo1–P | Mo2–P | P–N | N–N | N–NR | N–Mo2 |
|---|---|---|---|---|---|---|---|---|
| **A1** | $CH_2Ph$ | 0 | 2.566 | 2.585 | 1.686 | 1.323 | 1.279 | |
| **A2** | 4-$C_6H_4F$ | 0 | 2.557 | 2.586 | 1.687 | 1.323 | 1.290 | |
| **A3** | 4-$C_6H_4Me$ | 0 | 2.556 | 2.586 | 1.686 | 1.323 | 1.289 | |
| **B1** | $CH_2Ph$ | −18 | 2.591 | 2.647 | 1.749 | 1.292 | 1.291 | |
| **B2** | 4-$C_6H_4F$ | −20 | 2.577 | 2.647 | 1.766 | 1.278 | 1.301 | |
| **B3** | 4-$C_6H_4Me$ | −16 | 2.577 | 2.644 | 1.766 | 1.278 | 1.301 | |
| **C1** | $CH_2Ph$ | −22 | 2.595 | 2.427 | 1.772 | 1.266 | 1.329 | 2.280 |
| **C2** | 4-$C_6H_4F$ | +11 | 2.574 | 2.428 | 1.767 | 1.260 | 1.340 | 2.360 |
| **C3** | 4-$C_6H_4Me$ | +5 | 2.576 | 2.427 | 1.767 | 1.261 | 1.339 | 2.360 |
| **D1** | $CH_2Ph$ | −32 | 2.581 | 2.446 | 1.769 | 1.268 | 1.320 | 2.287 |
| **D2** | 4-$C_6H_4F$ | −19 | 2.597 | 2.440 | 1.758 | 1.266 | 1.336 | 2.329 |
| **D3** | 4-$C_6H_4Me$ | −25 | 2.600 | 2.439 | 1.758 | 1.266 | 1.335 | 2.329 |
| **E1** | $CH_2Ph$ | −207 | 2.545 | 2.662 | 1.601 | | | |
| **E2** | 4-$C_6H_4F$ | −214 | 2.574 | 2.669 | 1.610 | | | |
| **E3** | 4-$C_6H_4Me$ | −214 | 2.576 | 2.670 | 1.609 | | | |

[a] Energies relative to the structure of type **A** in each case, taking into account the release of CO (for structures **C** and **D**) or $N_2$ (for **E**); Mo2 refers to the atom in the MoCo(CO)x($PMe_3$) fragment (x = 1, 2).

As it can be concluded from the data in Table 5, the decarbonylation pathway leading to the metallacyclic complexes in the reactions with benzyl azide (**A1** →**B1** → **C1** + CO → **D1** + CO) is a downhill process in the thermodynamic sense, in agreement with the experimental findings and $^{31}$P NMR monitoring experiments discussed above. The denitrogenation pathway (**A1** → **B1** → **E1** + $N_2$) leading to the phosphaimine complex **E1** would be much more favored thermodynamically, thanks to the extrusion of the very stable $N_2$ molecule, but it seems to be kinetically more demanding (as no derivatives of **E1** are ever obtained upon methylation), thus allowing for the less favored decarbonylation route to prevail. For aryl azides, however, the formation of intermediates of type **C** (plus CO) is disfavored by some 20 to 30 kJ/mol with respect to the corresponding intermediate **B**, seemingly because of increased steric repulsions between the aryl group (compared to the benzyl group) and the MoCp(CO)($PMe_3$) fragment. This is reflected in the computed Mo−N distances of 2.360 Å for such intermediates (**C2** and **C3**), substantially longer than the corresponding value computed for the benzyl azide intermediate **C1** (2.280 Å). This circumstance might prevent intermediates **B2** and **B3** from undergoing an effective decarbonylation, then enabling the thermodynamically more favored (even if slower) denitrogenation route to prevail. In summary, we conclude that the phosphaimine derivatives **E** are the thermodynamic products of the reactions of **1** with all organic azides investigated, but that an alternative route involving decarbonylation at the $Mo(CO)_2$ center, along with N−Mo bond formation to give a PNNNMo cycle, is kinetically favored for the benzyl azide reaction, while disfavored for aryl azides because of increased steric repulsions between the aryl groups and the Mo(CO) center in the phosphatriazametallacyclic structure.

## Concluding Remarks

In its reactions with diazoalkanes, the electron-precise nature of compound **1** and the good nucleophilic properties of its phosphinidene ligand enable a fast nucleophilic attack of the P atom to the terminal N atom of the organic molecule, to give the corresponding *P*:*P*-bridged phosphadiazadiene derivatives, which are stabilized through protonation or methylation at the P-bound N atom, and show no tendency for denitrogenation. In a similar way, compound **1** reacts rapidly with different organic azides to give the corresponding *P*:*P*-bridged phosphatriazadiene derivatives, as result of nucleophilic attack of the phosphinidene ligand to the terminal N atom of the azide. These complexes, however, evolve rapidly at low temperature to give products depending on the azide used. For aryl azides 4-$C_6H_4X$ (X = Me, OMe), fast denitrogenation takes place at low temperature to give the corresponding phosphaimine-bridged complex, which can be stabilized through protonation or methylation at its N atom. For benzyl azide, the *P*:*P*-bridged phosphatriazadiene complex initially formed, which can be stabilized through methylation at the remote NR nitrogen at 223 K, evolve upon warming through a decarbonylation route involving coordination of the remote NR nitrogen to the MoCp fragment, to give unprecedented phosphatriazametallacyclic complexes which are stabilized through methylation at the P-bound N atom. DFT calculations indicate that the thermodynamic products of the reactions of **1** with all organic azides investigated are the corresponding phosphaimine derivatives. However, the alternative route involving decarbonylation at the $Mo(CO)_2$ center, along with N–Mo bond formation to give a PNNNMo cycle, seems kinetically favored for the benzyl azide reaction, but disfavored for aryl azides because of increased steric repulsions between the aryl groups and the Mo(CO) center in the phosphatriazametallacyclic structure.

## Experimental Section

**General Procedures and Starting Materials.** All manipulations and reactions were carried out under an argon (99.995%) atmosphere using standard Schlenk techniques. Solvents were purified according to literature procedures, and distilled prior to use.[30] Compound $[Mo_2Cp(\mu\text{-}\kappa^1{:}\kappa^1,\eta^5\text{-}PC_5H_4)(\eta^6\text{-}HMes^*)(CO)_2(PMe_3)]$ (**1**) was prepared in situ as described previously,[11] typically upon addition of stoichiometric amounts of $PMe_3$ on toluene solutions of $[Mo_2Cp(\mu\text{-}\kappa^1{:}\kappa^1,\eta^5\text{-}PC_5H_4)(\eta^6\text{-}HMes^*)(CO)_2]$,[12] in a Schlenk tube equipped with a Young´s valve. Reagents $N_2CPh_2$,[31] $Et_2O$ solutions of $N_2CH_2$,[32] $Na(BAr'_4)$,[33] and $[H(OEt_2)_2](BAr'_4)$,[34] were prepared as described previously [Mes* = 2,4,6-$C_6H_2{}^tBu_3$; Ar'= 3,5-$C_6H_3(CF_3)_2$]. All other reagents were obtained from commercial suppliers and used as received, unless otherwise stated. Petroleum ether refers to that fraction distilling in the range 338-343 K. Filtrations were carried out through diatomaceous earth unless otherwise stated. Chromatographic separations were carried out using jacketed columns cooled by tap water (ca. 288 K) or by a closed 2-propanol circuit kept at the desired temperature with a cryostat. Commercial aluminum oxide (activity I, 70-290 mesh) was degassed under vacuum prior to use. The latter was mixed under argon with the appropriate amount of water to reach activity IV. IR stretching frequencies of CO ligands were measured in solution (using $CaF_2$ windows), are referred to as $\nu$(CO), and are given in wave numbers ($cm^{-1}$). Nuclear magnetic resonance (NMR) spectra were routinely recorded at 295 K in $CD_2Cl_2$ solution unless otherwise stated. Chemical shifts ($\delta$) are given in ppm, relative to internal tetramethylsilane ($^1H$, $^{13}C$), or external 85% aqueous $H_3PO_4$ solutions ($^{31}P$). Coupling constants ($J$) are given in hertz.

**Preparation of $[Mo_2Cp\{\mu\text{-}\kappa^1_P{:}\kappa^1_P,\eta^5\text{-}P(NHNCH_2)C_5H_4\}(\eta^6\text{-}HMes^*)(CO)_2(PMe_3)](BAr'_4)$ (2a).** Excess $CH_2N_2$ (ca. 1 mL of a 0.6 M solution in $Et_2O$, ca. 0.6 mmol) was added to a toluene solution (2 mL) of compound **1**, prepared in situ from $[Mo_2Cp(\mu\text{-}\kappa^1{:}\kappa^1,\eta^5\text{-}PC_5H_4)(\eta^6\text{-}HMes^*)(CO)_2]$ (0.020 g, 0.031 mmol) at 253 K, and the mixture was stirred while allowing it to reach room temperature, to give a red solution. Then, solid $[H(OEt_2)_2](BAr'_4)$ (0.032 g, 0.031 mmol) was added, and the mixture was stirred for 1 min to give a green suspension. After removal of volatiles under vacuum, the residue was dissolved in dichloromethane (2 mL), and the solution was chromatographed on alumina at 253 K. Elution with dichloromethane/petroleum ether (1/2) gave a green fraction yielding, after removal of solvents, compound **1a** as a green microcrystalline solid (0.033 g, 65%). No microanalytical data were obtained for this very air-sensitive solid. $^1$H NMR (400.13 MHz, $CD_2Cl_2$, 233 K): $\delta$ 7.73 (s, 8H, Ar'), 7.57 (s, 4H, Ar'), 6.53, 6.10 (2d, $J_{HH}$ = 11, 2 x 1H, $CH_2$), 5.91 (d, $J_{HP}$ = 16, 1H, NH), 5.37 (d, $J_{HP}$ = 1.5, 5H, Cp), 5.19 (m, 2H, $C_5H_4$), 4.97 (m, 1H, $C_5H_4$), 4.92 (d, $J_{HP}$ = 4, 3H, $C_6H_3$), 4.07 (m, 1H, $C_5H_4$), 1.64 (d, $J_{HP}$ = 10, 9H, PMe), 1.20 (s, 27H, $^t$Bu). $^{13}$C{$^1$H} NMR (100.63 MHz, $CD_2Cl_2$, 233 K): $\delta$ 235.7 (t, $J_{CP}$ = 28, MoCO), 231.8 (t, $J_{CP}$ = 28, MoCO), 162.2 [q, $J_{CB}$ = 50, C$^1$(Ar')], 135.2 [s, C$^2$(Ar')], 129.7 (d, $J_{CP}$ = 11, N=$CH_2$), 129.4 [q, $J_{CF}$ = 32, C$^3$(Ar')], 125.0 (q, $J_{CF}$ = 272, $CF_3$), 117.9 [s, C$^4$(Ar')], 113.8 [s, C($C_6H_3$)], 93.5 (s, Cp), 92.9 [d, $J_{CP}$ = 14, C$^1$($C_5H_4$)], 90.3 [d, $J_{CP}$ = 8, CH($C_5H_4$)], 88.4 [d, $J_{CP}$ = 4, CH($C_5H_4$)], 82.7 [s, CH($C_5H_4$)], 78.2 [d, $J_{CP}$ = 17, CH($C_5H_4$)], 72.5 [s, CH($C_6H_3$)], 35.3 [s, C$^1$($^t$Bu)], 31.2 [s, C$^2$($^t$Bu)], 20.2 (d, $J_{CP}$ = 34, PMe).

**Preparation of [$Mo_2$Cp{$\mu$-$\kappa^1_P$:$\kappa^1_P$,$\eta^5$-P(NHNC$Ph_2$)$C_5H_4$}($\eta^6$-HMes*)$(CO)_2$($PMe_3$)](BAr'$_4$) (2b).** A 0.079 M solution of $N_2CPh_2$ in $Et_2O$ (1 mL, 0.079 mmol) was added to a toluene solution (2 mL) of compound **1**, prepared in situ from [$Mo_2$Cp($\mu$-$\kappa^1$:$\kappa^1$,$\eta^5$-P$C_5H_4$)($\eta^6$-HMes*)$(CO)_2$] (0.020 g, 0.031 mmol) at 253 K, and the mixture was stirred while allowing it to reach room temperature, to give a deep red solution. Then, solid [H($OEt_2$)$_2$](BAr'$_4$) (0.032 g, 0.031 mmol) was added, and the mixture was stirred for 1 min to give a green suspension. After removal of volatiles under vacuum, the residue was dissolved in dichloromethane (2 mL), and the solution was chromatographed on alumina at 263 K. Elution with dichloromethane/petroleum ether (1/1) gave a green fraction yielding, after removal of solvents, compound **1b** as a green microcrystalline solid (0.039 g, 70%). The crystals used in the X-ray diffraction study of **1b** were grown by the slow diffusion of layers of diethyl ether and petroleum ether into a concentrated dichloromethane solution of the complex at 253 K. Anal. Calcd for $C_{78}H_{71}BF_{24}Mo_2N_2O_2P_2$: C, 52.37; H, 4.00; N, 1.57. Found: C, 52.56; H, 4.25; N, 1.88. $^1$H NMR (400.13 MHz, $CD_2Cl_2$): $\delta$ 7.73 (s, 8H, Ar'), 7.57 (s, 4H, Ar'), 7.41-7.18 (m, 10H, Ph), 5.90 (d, $J_{HP}$ = 20, 1H, NH), 5.51 (s, 5H, Cp), 5.13 (m, 2H, $C_5H_4$), 4.79 (m, 1H, $C_5H_4$), 4.68 (d, $J_{HP}$ = 4, 3H, $C_6H_3$), 4.07 (m, 1H, $C_5H_4$), 1.66 (d, $J_{HP}$ = 10, 9H, PMe), 1.06 (s, 27H, $^t$Bu). $^{13}$C{$^1$H} NMR (100.63 MHz, $CD_2Cl_2$): $\delta$ 235.7 (t, $J_{CP}$ = 28, MoCO), 231.6 (m, MoCO), 162.2 [q, $J_{CB}$ = 50, C$^1$(Ar')], 148.5 (d, $J_{CP}$ = 10, N=C), 138.4 [s, C$^1$(Ph)], 135.2 [s, C$^2$(Ar')], 133.2 [s, C$^1$(Ph)], 131.7-126.9 (Ph), 129.3 [q, $J_{CF}$ = 32, C$^3$(Ar')], 125.0 (q, $J_{CF}$ = 273, $CF_3$), 117.9 [s, C$^4$(Ar')], 113.7 [s, C($C_6H_3$)], 93.8 [d, $J_{CP}$ = 34, C$^1$($C_5H_4$)], 93.5 (s, Cp), 90.1 [d, $J_{CP}$ = 8, CH($C_5H_4$)], 88.7 [d, $J_{CP}$ = 4,

$CH(C_5H_4)$], 82.1 [s, $CH(C_5H_4)$], 78.0 [d, $J_{CP}$ = 17, $CH(C_5H_4)$], 72.1 [s, $CH(C_6H_3)$], 35.2 [s, $C^1$($^t$Bu)], 31.2 [s, $C^2$($^t$Bu)], 20.3 (d, $J_{CP}$ = 34, PMe).

**Preparation of [$Mo_2$Cp{$\mu$-$\kappa^1_P$:$\kappa^1_P$,$\eta^5$-P(NHNCHC$O_2$Et)$C_5H_4$}($\eta^6$-HMes*)$(CO)_2$($PMe_3$)](BAr'$_4$) (2c).** The procedure is completely similar to the one described for **2b**, except that neat $N_2CHCO_2Et$ (8 $\mu$L, 0.076 mmol) was used instead. After similar workup, compound **2c** was isolated as a green microcrystalline solid (0.039 g, 74%). No microanalytical data were obtained for this very air-sensitive solid. $^1$H NMR (400.13 MHz, $CD_2Cl_2$): $\delta$ 7.73 (s, 8H, Ar'), 7.57 (s, 4H, Ar'), 6.98 (d, $J_{HP}$ = 1, 1H, CH), 6.54 (d, $J_{HP}$ = 18, 1H, NH), 5.47 (d, $J_{HP}$ = 2, 5H, Cp), 5.21 (m, 2H, $C_5H_4$), 4.98 (d, $J_{HP}$ = 4, 3H, $C_6H_3$), 4.96 (m, 1H, $C_5H_4$), 4.25 (q, $J_{HH}$ = 7, 2H, $OCH_2$), 4.14 (m, 1H, $C_5H_4$), 1.65 (d, $J_{HP}$ = 10, 9H, PMe), 1.30 (t, $J_{HH}$ = 7, 3H, $CH_3$), 1.20 (s, 27H, $^t$Bu). $^{13}C\{^1H\}$ NMR (100.63 MHz, $CD_2Cl_2$): $\delta$ 235.7 (t, $J_{CP}$ = 28, MoCO), 231.8 (t, $J_{CP}$ = 28, MoCO), 163.5 (s, $CO_2$Et), 162.2 [q, $J_{CB}$ = 50, $C^1$(Ar')], 135.3 [s, $C^2$(Ar')], 130.0 (d, $J_{CP}$ = 10, N=CH), 129.3 [q, $J_{CF}$ = 32, $C^3$(Ar')], 125.0 (q, $J_{CF}$ = 273, $CF_3$), 117.9 [s, $C^4$(Ar')], 114.4 [s, $C(C_6H_3)$], 94.0 (s, Cp), 92.9 [d, $J_{CP}$ = 32, $C^1(C_5H_4)$], 90.3 [d, $J_{CP}$ = 8, $CH(C_5H_4)$], 88.4 [d, $J_{CP}$ = 4, $CH(C_5H_4)$], 82.1 [s, $CH(C_5H_4)$], 77.9 [d, $J_{CP}$ = 18, $CH(C_5H_4)$], 73.0 [s, $CH(C_6H_3)$], 61.4 (s, $OCH_2$), 35.4 [s, $C^1$($^t$Bu)], 31.2 [s, $C^2$($^t$Bu)], 20.3 (d, $J_{CP}$ = 34, PMe), 14.5 (s, $CH_3$).

**Preparation of [$Mo_2$Cp{$\mu$-$\kappa^1_P$:$\kappa^1_P$,$\eta^5$-P(NMeNCHC$O_2$Et)$C_5H_4$}($\eta^6$-HMes*)$(CO)_2$($PMe_3$)](BAr'$_4$) (3).** Neat $N_2CHCO_2Et$ (8 $\mu$L, 0.076 mmol) was added to a toluene solution (2 mL) of compound **1**, prepared in situ from [$Mo_2$Cp($\mu$-$\kappa^1$:$\kappa^1$,$\eta^5$-$PC_5H_4$)($\eta^6$-HMes*)$(CO)_2$] (0.020 g, 0.031 mmol) at 263 K, and the mixture was stirred at this temperature for 1 min, to give a brown-greenish solution. Then, neat MeI (10 $\mu$L, 0.160 mmol) was added, and the mixture was stirred at the same temperature for a further 2 min, to give a green suspension. After removal of volatiles, the residue was dissolved in dichloromethane (2 mL), then solid Na(BAr'$_4$) (0.027 g, 0.031 mmol) was added, and the mixture was stirred at room temperature for 5 min, then chromatographed on alumina at 263 K. Elution with dichloromethane/petroleum ether (1/1) gave a green fraction yielding, after removal of solvents, a green solid shown (by NMR) to contain a mixture of compounds **3** and **2c** in a ca. 2:1 ratio (0.029 g, yield of **3** ca. 37%), which could not be resolved. However, a small amount of crystals of **3**, suitable for an X-ray diffraction analysis, could be grown by the slow diffusion of a layer of petroleum ether into a concentrated dichloromethane solution of the above mixture at 253 K. Anal. Calcd for $C_{70}H_{69}BF_{24}Mo_2N_2O_4P_2$: C, 48.80; H, 4.04; N, 1.63. Found: C, 49.05; H, 3.99; N, 1.89. $^1$H NMR (400.13 MHz, $CD_2Cl_2$): $\delta$ 7.73 (s, 8H, Ar'), 7.56 (s, 4H, Ar'), 6.60 (s, 1H, CH), 5.51 (d, $J_{HP}$ = 1, 5H, Cp), 5.23, 5.13 (2m, 2 x 1H, $C_5H_4$), 4.97 (s, br, 3H, $C_6H_3$), 4.56 (m, 1H, $C_5H_4$), 4.26 (q, $J_{HH}$ = 7, 2H, $OCH_2$), 4.08

(m, 1H, $C_5H_4$), 3.37 (d, $J_{HP}$ = 5, 3H, NMe), 1.66 (d, $J_{HP}$ = 10, 9H, PMe), 1.31 (t, $J_{HH}$ = 7, 3H, $CH_3$), 1.22 (s, 27H, $^t$Bu).

**Preparation of [$Mo_2Cp\{\mu$-$\kappa^1_P:\kappa^1_P,\eta^5$-P(NH(4-$C_6H_4$Me))$C_5H_4\}(\eta^6$-HMes*)$(CO)_2(PMe_3)$](BAr'$_4$) (4d).** A 0.5 M solution of azide $N_3$(4-$C_6H_4$Me) in toluene (62 $\mu$L, 0.031 mmol) was added to a toluene solution (2 mL) of compound **1**, prepared in situ from [$Mo_2Cp(\mu$-$\kappa^1:\kappa^1,\eta^5$-$PC_5H_4)(\eta^6$-HMes*)$(CO)_2$] (0.020 g, 0.031 mmol) at 253 K, and the mixture was stirred for 1 min to give a brown-greenish suspension. After removal of the solvent under vacuum, the residue was dissolved in dichloromethane (2 mL). Then, solid [$H(OEt_2)_2$](BAr'$_4$) (0.032 g, 0.031 mmol) was added, and the mixture was stirred for 5 min to give a green solution, which was chromatographed on alumina at 263 K. Elution with dichloromethane/petroleum ether (2/3) gave a green fraction yielding, after removal of solvents, compound **4d** as a green microcrystalline solid (0.036 g, 68%). No microanalytical data were obtained for this very air-sensitive solid. $^1$H NMR (400.13 MHz, $CD_2Cl_2$, 233 K): $\delta$ 7.78 (s, 8H, Ar'), 7.60 (s, 4H, Ar'), 7.13, 6.97 (2d, $J_{HH}$ = 8, 2 x 2H, $C_6H_4$), 5.24, 5.21, 5.12 (3m, 3 x 1H, $C_5H_4$), 4.99 (s, 5H, Cp), 4.86 (s, 3H, $C_6H_3$), 4.13 (d, $J_{HP}$ = 13, 1H, NH), 3.88 (m, 1H, $C_5H_4$), 2.29 (s, 3H, Me), 1.53 (d, $J_{HP}$ = 9, 9H, PMe), 1.23 (s, 27H, $^t$Bu). $^{13}$C{$^1$H} NMR (100.63 MHz, $CD_2Cl_2$, 233 K): $\delta$ 235.1 (s, br, 2MoCO), 162.1 [q, $J_{CB}$ = 50, C$^1$(Ar')], 140.7 [d, $J_{CP}$ = 12, C$^1$($C_6H_4$)], 135.0 [s, C$^2$(Ar')], 131.9 [s, C$^4$($C_6H_4$)], 130.0 [s, C$^{2,3}$($C_6H_4$)], 129.1 [q, $J_{CF}$ = 32, C$^3$(Ar')], 128.9 [s, C$^{2,3}$($C_6H_4$)], 124.9 (q, $J_{CF}$ = 272, $CF_3$), 117.9 [s, C$^4$(Ar')], 113.0 [s, C($C_6H_3$)], 97.3 [s, br, C$^1$($C_5H_4$)], 92.8 (s, Cp), 90.2 [d, $J_{CP}$ = 7, CH($C_5H_4$)], 88.6 [d, $J_{CP}$ = 3, CH($C_5H_4$)], 83.6 [s, CH($C_5H_4$)], 78.9 [d, $J_{CP}$ = 18, CH($C_5H_4$)], 72.0 [s, CH($C_6H_3$)], 35.3 [s, C$^1$($^t$Bu)], 31.2 [s, C$^2$($^t$Bu)], 20.9 (s, Me), 20.0 (d, $J_{CP}$ = 34, PMe).

**Preparation of [$Mo_2Cp\{\mu$-$\kappa^1_P:\kappa^1_P,\eta^5$-P(NH(4-$C_6H_4$F))$C_5H_4\}(\eta^6$-HMes*)$(CO)_2(PMe_3)$](BAr'$_4$) (4e).** The procedure is completely analogous to the one just described for compound **4d**, except that azide $N_3$(4-$C_6H_4$F) (62 $\mu$L of a 0.5 M solution in toluene, 0.031 mmol) was used instead. After similar workup (elution with dichloromethane/petroleum ether (1/2)) a green microcrystalline solid was obtained (0.041 g, 78%). No microanalytical data were obtained for this very air-sensitive solid. $^1$H NMR (400.13 MHz, $CD_2Cl_2$): $\delta$ 7.73 (s, 8H, Ar'), 7.57 (s, 4H, Ar'), 7.04, 7.02 (AB mult, 2 x 2H, $C_6H_4$), 5.23 (m, 2H, $C_5H_4$), 5.08 (m, 1H, $C_5H_4$), 5.04 (s, 5H, Cp), 4.89 (d, $J_{HP}$ = 4, 3H, $C_6H_3$), 4.09 (d, $J_{HP}$ = 13, 1H, NH), 3.92 (m, 1H, $C_5H_4$), 1.52 (d, $J_{HP}$ = 10, 9H, PMe), 1.24 (s, 27H, $^t$Bu). $^{13}$C{$^1$H} NMR (100.63 MHz, $CD_2Cl_2$): $\delta$ 235.4 (t, $J_{CP}$ = 28, MoCO), 234.3 (t, $J_{CP}$ = 38, CO), 162.2 [q, $J_{CB}$ = 50, C$^1$(Ar')], 159.7 [d, $J_{CF}$ = 243, C$^4$($C_6H_4$)], 139.6 [dd, $J_{CP}$ = 13, $J_{CF}$ = 2, C$^1$($C_6H_4$)], 135.2 [s, C$^2$(Ar')], 129.3 [q, $J_{CF}$ = 32, C$^3$(Ar')], 125.0 (q, $J_{CF}$ = 272, $CF_3$), 125.0 [m, C$^2$($C_6H_4$)], 117.9 [s, C$^4$(Ar')], 116.2 [d, $J_{CF}$ = 23, C$^3$($C_6H_4$)], 113.7 [s, C($C_6H_3$)], 97.2 [d, $J_{CP}$ = 25, C$^1$($C_5H_4$)], 92.9 (s, Cp), 90.2 [d, $J_{CP}$ = 8, CH($C_5H_4$)], 88.7 [d, $J_{CP}$ = 4, CH($C_5H_4$)], 83.4 [s, CH($C_5H_4$)], 78.8 [d, $J_{CP}$ = 18, CH($C_5H_4$)], 72.5 [s, CH($C_6H_3$)], 35.4 [s, $C^1$($^t$Bu)], 31.3 [s, $C^2$($^t$Bu)], 20.1 (d, $J_{CP}$ = 34, PMe).

**Preparation of [$Mo_2$Cp{$\mu$-$\kappa^1_P$:$\kappa^1_P$,$\eta^5$-P(NMe(4-$C_6H_4$F))$C_5H_4$}($\eta^6$-HMes*)(CO)$_2$(PMe$_3$)](BAr'$_4$) (5).** A 0.5 M solution of azide $N_3$(4-$C_6H_4$F) in toluene (62 $\mu$L, 0.031 mmol) was added to a toluene solution (2 mL) of compound **1**, prepared in situ from [$Mo_2$Cp($\mu$-$\kappa^1$:$\kappa^1$,$\eta^5$-P$C_5H_4$)($\eta^6$-HMes*)(CO)$_2$] (0.020 g, 0.031 mmol) at 253 K, and the mixture was stirred for 1 min to give a brown-greenish suspension. Then, neat MeI (10 $\mu$L, 0.160 mmol) was added, and the mixture was stirred at the same temperature for 5 min, to give a green suspension. After removal of the solvent under vacuum, the residue was dissolved in dichloromethane (1 mL), and solid Na(BAr'$_4$) (0.027 g, 0.031 mmol) was added, and the mixture was stirred at room temperature for 5 min to give a green solution, which was chromatographed on alumina at 263 K. Elution with dichloromethane/petroleum ether (1/2) gave a green fraction yielding, after removal of solvents, an air-sensitive green solid shown (by NMR) to contain a mixture of compounds **5** and **4e** in a ca. 2:1 ratio (0.030 g, yield of **5** ca. 38%), which could not be further purified. *Spectroscopic data for compound **5***: $^1$H NMR (400.13 MHz, $CD_2Cl_2$): $\delta$ 7.73 (s, 8H, Ar'), 7.57 (s, 4H, Ar'), 7.09, 7.03 (2d, $J_{HH}$ = 8, 2 x 2H, $C_6H_4$), 5.18, 5.15, 4.90 (3m, 3 x 1H, $C_5H_4$), 4.86 (d, $J_{HP}$ = 1, 5H, Cp), 3.88 (m, 1H, $C_5H_4$), 3.32 (d, $J_{HP}$ = 10, 3H, NMe), 1.54 (d, $J_{HP}$ = 10, 9H, PMe), 1.25 (s, 27H, $^t$Bu). $^{13}$C{$^1$H} NMR (100.63 MHz, $CD_2Cl_2$): $\delta$ 236.0 (br, MoCO), 234.7 (m, MoCO), 162.2 [q, $J_{CB}$ = 50, $C^1$(Ar')], 159.9 [d, $J_{CF}$ = 244, $C^4$($C_6H_4$)], 145.6 [m, $C^1$($C_6H_4$)], 135.2 [s, $C^2$(Ar')], 129.3 [q, $J_{CF}$ = 32, $C^3$(Ar')], 127.1 [m, $C^2$($C_6H_4$)], 125.0 (q, $J_{CF}$ = 272, $CF_3$), 117.9 [s, $C^4$(Ar')], 116.2 [d, $J_{CF}$ = 22, $C^3$($C_6H_4$)], 113.7 [C($C_6H_3$)], 92.5 (s, Cp), 90.0 [d, $J_{CP}$ = 7, CH($C_5H_4$)], 87.1 [s, br, CH($C_5H_4$)], 83.2 [s, CH($C_5H_4$)], 78.0 [d, $J_{CP}$ = 18, $C^1$($C_5H_4$)], 76.4 [s, CH($C_5H_4$)], 72.5 [s, CH($C_6H_3$)], 49.8 (m, NMe), 35.4 [s, $C^1$($^t$Bu)], 31.5 [s, $C^2$($^t$Bu)], 20.2 (d, $J_{CP}$ = 34, PMe).

**Preparation of [$Mo_2$Cp{$\mu$-$\kappa^1_P$:$\kappa^1_P$,$\eta^5$-P(NHCH$_2$Ph)$C_5H_4$}($\eta^6$-HMes*)(CO)$_2$(PMe$_3$)](BAr'$_4$) (4f).** Neat benzyl azide (9 $\mu$L, 0.066 mmol) was added to a toluene solution (2 mL) of compound **1**, prepared in situ from [$Mo_2$Cp($\mu$-$\kappa^1$:$\kappa^1$,$\eta^5$-P$C_5H_4$)($\eta^6$-HMes*)(CO)$_2$] (0.020 g, 0.031 mmol) at 253 K, and the mixture was stirred for 1 min to give a red solution. Then solid ($NH_4$)$PF_6$ (0.025 g, 0.153 mmol) was added, and the mixture was stirred while allowed to reach room temperature slowly, to give a brown solution. After removal of the solvent under vacuum, the residue was dissolved in dichloromethane (2 mL) and the solution was filtered using a canula. Then, solid Na(BAr'$_4$) (0.027 g, 0.031 mmol) was added to the filtrate, and the mixture was stirred for 5 min, then chromatographed on alumina at 263 K. Elution with dichloromethane/petroleum ether (1/2) gave a brown fraction yielding, after removal of solvents, compound **4f** as a brown microcrystalline solid (0.023 g, 44%). No microanalytical data were obtained for this very air-sensitive solid. $^{1}$H NMR (300.13 MHz, $CD_2Cl_2$): $\delta$ 7.73 (s, 8H, Ar'), 7.57 (s, 4H, Ar'), 7.32 (m, 5H, Ph), 5.37 (d, $J_{HP}$ = 1, 5H, Cp), 5.15 (m, 2H, $C_5H_4$), 4.94 (m, 1H, $C_5H_4$), 4.86 (d, $J_{HP}$ = 4, 3H, $C_6H_3$), 4.22 (td, $J_{HH}$ = $J_{HP}$ = 14, $J_{HH}$ = 8, 1H, $CH_2$), 4.00 (td, $J_{HH}$ = $J_{HP}$ = 14, $J_{HH}$ = 5, 1H, $CH_2$), 3.91 (m, 1H, $C_5H_4$), 2.15 (m, 1H, NH), 1.68 (d, $J_{HP}$ = 10, 9H, PMe), 1.19 (s, 27H, $^{t}$Bu).

**Preparation of [$Mo_2Cp\{\mu\text{-}\kappa^1_P:\kappa^1_P,\eta^5\text{-}P(NNNMeCH_2Ph)C_5H_4\}(\eta^6$-HMes*)$(CO)_2(PMe_3)$](BAr'$_4$) (6).** Neat benzyl azide (9 $\mu$L, 0.066 mmol) was added to a toluene solution (2 mL) of compound **1**, prepared in situ from [$Mo_2Cp(\mu\text{-}\kappa^1:\kappa^1,\eta^5\text{-}PC_5H_4)(\eta^6$-HMes*)$(CO)_2$] (0.020 g, 0.031 mmol) at 223 K, and the mixture was stirred for 1 min to give a green solution. Then neat MeI (10 $\mu$L, 0.160 mmol) was added, and the mixture was stirred while allowed to reach room temperature slowly, to give a brown-greenish suspension. After removal of volatiles under vacuum, the residue was dissolved in dichloromethane (2 mL), then solid Na(BAr'$_4$) (0.027 g, 0.031 mmol) was added, and the mixture was stirred for 1 min, then chromatographed on alumina at 253 K. Elution with dichloromethane/petroleum ether (1/3) gave a green fraction yielding, after removal of solvents, compound **6** as a green microcrystalline solid (0.038 g, 70%). The crystals used in the X-ray diffraction study of **6** were grown by the slow diffusion of a layer of petroleum ether into a concentrated dichloromethane solution of the complex at 253 K. Anal. Calcd for $C_{73}H_{70}BF_{24}Mo_2N_3O_2P_2$: C, 50.33; H, 4.05; N, 2.41. Found: C, 50.56; H, 4.20; N, 2.68. $^{1}$H NMR (400.13 MHz, $CD_2Cl_2$, 233 K): $\delta$ 7.77 (s, 8H, Ar'), 7.60 (s, 4H, Ar'), 7.37 (m, 3H, Ph), 7.21 (m, 2H, Ph), 5.43, 5.27 (2m, 2 x 1H, $C_5H_4$), 5.24 (d, $J_{HP}$ = 1, 5H, Cp), 5.07, 4.88 (2d, $J_{HH}$ = 15, 2 x 1H, $CH_2$), 4.76 (d, $J_{HP}$ = 4, 3H, $C_6H_3$), 4.74, 4.41 (2m, 2 x 1H, $C_5H_4$), 2.92 (s, 3H, NMe), 1.64 (d, $J_{HP}$ = 10, 9H, PMe), 1.15 (s, 27H, $^{t}$Bu). $^{13}C\{^{1}H\}$ NMR (100.63 MHz, $CD_2Cl_2$, 233 K): $\delta$ 235.7 (dd, $J_{CP}$ = 28, 22, MoCO), 232.6 (dd, $J_{CP}$ = 28, 24, MoCO), 162.1 [q, $J_{CB}$ = 50, $C^1$(Ar')], 136.9 [s, $C^1$(Ph)], 135.0 [s, $C^2$(Ar')], 129.1 [s, $C^{2,3}$(Ph)], 129.0 [q, $J_{CF}$ = 32, $C^3$(Ar')], 128.4 [s, $C^4$(Ph)], 128.0 [s, $C^{2,3}$(Ph)], 124.8 (q, $J_{CF}$ = 272, $CF_3$), 117.9 [s, $C^4$(Ar')], 112.3 [s, C($C_6H_3$)], 94.8 [d, $J_{CP}$ = 9, $C^1$($C_5H_4$)], 92.6 (s, Cp), 90.1 [d, $J_{CP}$ = 9, CH($C_5H_4$)], 87.8 [s, br, CH($C_5H_4$)], 85.4 [s, CH($C_5H_4$)], 80.9 [d, $J_{CP}$ = 16, CH($C_5H_4$)], 71.9 [s, CH($C_6H_3$)], 60.0 (s, $CH_2$), 35.1 [s, $C^1$($^{t}$Bu)], 34.3 (s, NMe), 31.1 [s, $C^2$($^{t}$Bu)], 19.5 (d, $J_{CP}$ = 33, PMe).

**Preparation of *syn*-[$Mo_2Cp\{\mu\text{-}\kappa^2_{P,N}:\kappa^1_P,\eta^5\text{-}P(NMeNNCH_2Ph)C_5H_4\}(\eta^6$-HMes*)(CO)$(PMe_3)$](BAr'$_4$) (*syn*-7).** Neat benzyl azide (9 $\mu$L, 0.066 mmol) was added to a toluene solution (2 mL) of compound **1**, prepared in situ from [$Mo_2Cp(\mu\text{-}\kappa^1:\kappa^1,\eta^5\text{-}PC_5H_4)(\eta^6$-HMes*)$(CO)_2$] (0.020 g, 0.031 mmol) at 253 K, and the mixture was stirred for 1 min to give a red solution. Then neat MeI (10 $\mu$L, 0.160 mmol) was added, and the mixture was stirred while allowed to reach room temperature slowly, to give a brown-greenish suspension. After removal of volatiles under vacuum, the residue was dissolved in dichloromethane (2 mL), then solid Na(BAr'$_4$) (0.027 g, 0.031 mmol) was added, and the mixture was stirred for 1 min, then chromatographed on alumina at 263 K. Elution with dichloromethane/petroleum ether (1/2) gave a red fraction yielding, after removal of solvents, compound ***syn*-7** as a green microcrystalline solid (0.036 g, 68%). Anal. Calcd for $C_{72}H_{70}BF_{24}Mo_2N_3OP_2$: C, 50.46; H, 4.12; N, 2.45. Found: C, 50.10; H, 4.41; N, 2.73. $^1$H NMR (400.13 MHz, $CD_2Cl_2$): $\delta$ 7.72 (s, 8H, Ar'), 7.56 (s, 4H, Ar'), 7.37 (m, 3H, Ph), 7.13 (m, 2H, Ph), 5.37 (m, 1H, $C_5H_4$), 5.28 (d, $J_{HH}$ = 14, 1H, $CH_2$), 5.18 (d, $J_{HP}$ = 3, 3H, $C_6H_3$), 5.00 (m, 1H, $C_5H_4$), 4.93 (s, 5H, Cp), 4.91 (m, 1H, $C_5H_4$), 4.90 (d, $J_{HH}$ = 14, 1H, $CH_2$), 3.80 (d, $J_{HP}$ = 1, 3H, NMe), 3.71 (m, 1H, $C_5H_4$), 1.55 (d, $J_{HP}$ = 9, 9H, PMe), 1.22 (s, 27H, $^t$Bu). $^{13}$C{$^1$H} NMR (100.63 MHz, $CD_2Cl_2$): $\delta$ 258.4 (dd, $J_{CP}$ = 37, 29, MoCO), 162.2 [q, $J_{CB}$ = 50, C$^1$(Ar')], 136.7 [s, C$^1$(Ph)], 135.2 [s, C$^2$(Ar')], 129.4 [s, C$^{2,3}$(Ph)], 129.1 [q, $J_{CF}$ = 32, C$^3$(Ar')], 128.8 [s, C$^4$(Ph)], 128.2 [s, C$^{2,3}$(Ph)], 124.8 (q, $J_{CF}$ = 272, $CF_3$), 117.9 [s, C$^4$(Ar')], 114.4 [s, br, C($C_6H_3$)], 91.7 (s, Cp), 90.1 [d, $J_{CP}$ = 2, CH($C_5H_4$)], 86.9 [d, $J_{CP}$ = 8, CH($C_5H_4$)], 85.2 [s, CH($C_5H_4$)], 79.4 [d, $J_{CP}$ = 47, C$^1$($C_5H_4$)], 74.7 [d, $J_{CP}$ = 18, CH($C_5H_4$)], 74.6 [s, CH($C_6H_3$)], 74.2 [d, $J_{CP}$ = 7, $CH_2$], 41.3 (s, NMe), 35.7 [s, C$^1$($^t$Bu)], 31.4 [s, C$^2$($^t$Bu)], 21.3 (d, $J_{CP}$ = 28, PMe).

**Preparation of *anti*-[Mo$_2$Cp{$\mu$-$\kappa^2_{P,N}$:$\kappa^1_P$,$\eta^5$-P(NMeNNCH$_2$Ph)C$_5$H$_4$}($\eta^6$-HMes*)(CO)(PMe$_3$)](BAr'$_4$) (*anti*-7).** The procedure is identical to the one described for isomer ***syn*-7**, except that MeI was added at room temperature. After similar workup (elution with dichloromethane/petroleum ether (1/1)), isomer ***anti*-7** was isolated as a red microcrystalline solid (0.043 g, 81%). The crystals used in the X-ray diffraction study of ***anti*-7** were grown by the slow diffusion of a layer of petroleum ether into a concentrated dichloromethane solution of the complex at 253 K. Anal. Calcd for $C_{72}H_{70}BF_{24}Mo_2N_3OP_2$: C, 50.46; H, 4.12; N, 2.45. Found: C, 50.34; H, 3.90; N, 2.59. $^1$H NMR (400.13 MHz, $CD_2Cl_2$, 233 K): $\delta$ 7.72 (s, 8H, Ar'), 7.56 (s, 4H, Ar'), 7.40 (m, 3H, Ph), 7.26 (m, 2H, Ph), 5.38 (m, 1H, $C_5H_4$), 5.35 (d, $J_{HH}$ = 12, 1H, $CH_2$), 5.21 (m, 1H, $C_5H_4$), 5.04 (s, 5H, Cp), 5.02 (m, 1H, $C_5H_4$), 4.93 (d, $J_{HP}$ = 2, 3H, $C_6H_3$), 4.76 (d, $J_{HH}$ = 12, 1H, $CH_2$), 4.02 (m, 1H, $C_5H_4$), 3.65 (d, $J_{HP}$ = 1, 3H, NMe), 1.62 (d, $J_{HP}$ = 9, 9H, PMe), 1.03 (s, 27H, $^t$Bu). $^{13}$C{$^1$H} NMR (100.63 MHz, $CD_2Cl_2$): $\delta$ 230.0 (s, br, MoCO), 162.1 [q, $J_{CB}$ = 50, C$^1$(Ar')], 136.0 [s, C$^1$(Ph)], 135.2 [s, C$^2$(Ar')], 130.2, 129.3 [2s, C$^{2,3}$(Ph)], 129.2 [s, C$^4$(Ph)], 129.1 [q, $J_{CF}$ = 32, C$^3$(Ar')], 125.0 (q, $J_{CF}$ = 272, $CF_3$), 117.9 [s, C$^4$(Ar')], 113.5 [s, C($C_6H_3$)], 92.3 (s, Cp), 90.5 [d, $J_{CP}$ = 5, CH($C_5H_4$)], 86.7 [d, $J_{CP}$ = 10, CH($C_5H_4$)], 85.5 [s, CH($C_5H_4$)], 75.1 [d, $J_{CP}$ = 28, CH($C_5H_4$)], 74.9 (s, $CH_2$), 73.7 [s, CH($C_6H_3$)], 72.3 [d, $J_{CP}$ = 8, C$^1$($C_5H_4$)], 40.9 (s, NMe), 35.0 [s, C$^1$($^t$Bu)], 31.1 [s, C$^2$($^t$Bu)], 20.1 (d, $J_{CP}$ = 29, PMe).

**X-Ray Structure Determination of Compounds 2b, 3 and 6.** Data collection for these compounds was performed at ca. 155 K on an Oxford Diffraction Xcalibur Nova single crystal diffractometer, using Cu K$\alpha$ radiation. Images were collected at a 62 mm fixed crystal-detector distance using the oscillation method, with 1.0-1.3º oscillation and variable exposure time per image. Data collection strategy was calculated with the program *CrysAlis Pro CCD*,[35] and data reduction and cell refinement was performed with the program *CrysAlis Pro RED*.[35] In all cases, an empirical absorption correction was applied using the SCALE3 ABSPACK algorithm as implemented in the program *CrysAlis Pro RED*. Using the program suite WinGX,[36] the structures were solved by Patterson interpretation and phase expansion using SHELXL2016,[37] and refined with full-matrix least squares on $F^2$ using SHELXL2016. In general, all non-hydrogen atoms were refined anisotropically, except for atoms involved in disorder, and all hydrogen atoms were geometrically placed and refined using a riding model, with a few exceptions detailed below. For compound **2b**, the N-bound H(1) atom was located in the Fourier maps and refined isotropically; besides this, the complex crystallized with a molecule of diethyl ether. The latter molecule and two $CF_3$ groups of the anion were somewhat disordered, but a satisfactory modeling could not be achieved. In compound **3** the anion displayed four $CF_3$ groups disordered, satisfactorily modeled over two positions with 0.5 occupancies; in this case, the C-bound H(4) atom was located in the Fourier maps and refined isotropically. In compound **6** the anion displayed four $CF_3$ groups disordered, satisfactorily modeled over two positions with 0.5 occupancies, and the benzyl group in the cation was also disordered over two sites, now modeled with 0.55/0.45 occupancies. In this case, a highly disordered molecule of a non-identified solvent was present in the crystal lattice; then, the SQUEEZE procedure,[38] as implemented in PLATON,[39] was used. Other data for the refinements of these structures can be found in the Supporting Information (Table S1).

**X-Ray Structure Determination of Compound *anti*-7.** Data collection for this compound was performed on a Kappa-Appex-II Bruker diffractometer using graphite-monochromated Mo$K_\alpha$ radiation at 100 K. The software APEX[40] was used for collecting frames with the $\omega/\phi$ scans measurement method. The Bruker SAINT software was used for the data reduction,[41] and a multi-scan absorption correction was applied with SADABS.[42] Structure solution and refinements were carried out as described above using SHELXL2016. In this case, four $CF_3$ groups in the anion were disordered and satisfactorily modeled over two sites, with 0.5 occupancies. The cyclopentadienyl ligand and the benzyl group in the cation were also somewhat disordered, but we could not achieve a satisfactory modeling for such disorder. In addition, a highly disordered molecule of a non-identified solvent was present in the crystal lattice, treated with the SQUEEZE procedure as described above.

**Computational Details**. All DFT calculations were carried out using the GAUSSIAN09 package,[43] and the M06L functional.[44] A pruned numerical integration grid (99,590) was used for all the calculations *via* the keyword Int=Ultrafine. Effective core potentials and their associated double-ζ LANL2DZ basis set were used for Mo atoms.[45] The light elements (P, F, O, N, C and H) were described with the 6-31G* basis.[46] Geometry optimizations were performed under no symmetry restrictions, using initial coordinates derived from the X-ray data. Frequency analysis was performed for all the stationary points to ensure that a minimum structure with no imaginary frequencies was achieved in each case.

**ASSOCIATED CONTENT**

**Supporting Information.** A PDF file containing crystal data for compounds **2b**, **3**, **6** and ***anti*-7**, a view of the cation in compound **3**, views of DFT-computed structures for intermediates **A2** to **E2** and **A3** to **E3**, and NMR spectra for all new compounds. An XYZ file including the Cartesian coordinates for all computed species. This material is available free of charge *via* the Internet at http://pubs.acs.org.

**AUTHOR INFORMATION**

**Corresponding Authors.** E-mail: garciavdaniel@uniovi.es (D. G. V.), mara@uniovi.es (M. A. R).

**Author Contribution.** The manuscript was written through contributions of all authors.

**Notes.** The authors declare no competing financial interests.

**ACKNOWLEDGMENTS**

We thank the MICINN of Spain and FEDER for financial support (Project PGC2018-097366-B-I00), the Universidad de Oviedo for a grant (to P.V.), the SCBI of the Universidad de Málaga, Spain, for access to computing facilities, and the X-Ray units of the Universidad de Oviedo and Universidad de Santiago de Compostela, Spain, for acquisition of diffraction data.

## References

1. Dillon, K. B.; Mathey, F.; Nixon, J. F. *Phosphorus: The Carbon-Copy*; Wiley: Chichester, 1998.
2. For some reviews, see: (a) Mathey, F.; Duan, Z. Activation of A−H bonds (A = B, C, N, O, Si) by using monovalent phosphorus complexes [RP→M]. *Dalton Trans.* **2016**, *45*, 1804-1809. (b) Aktas, H.; Slootweg, J. C.; Lammertsma, K. Nucleophilic phosphinidene complexes: access and applicability. *Angew. Chem. Int. Ed.* **2010**, *49*, 2102-2113. (c) Waterman, R. Metal-phosphido and -phosphinidene complexes in P−E bond-forming reactions. *Dalton Trans.* **2009**, 18-26. (d) Mathey, F. Developing the chemistry of monovalent phosphorus. *Dalton Trans.* **2007**, 1861-

1868. (e) Lammertsma, K. Phosphinidenes. *Top. Curr. Chem.* **2003**, *229*, 95-119. (f) Lammertsma, K.; Vlaar, M. J. M. Carbene-Like Chemistry of Phosphinidene Complexes − Reactions, Applications, and Mechanistic Insights. *Eur. J. Org. Chem.* **2002**, 1127-1138. (g) Streubel, R. Chemistry of $\lambda^3$-2*H*-azaphosphirene metal complexes. *Coord. Chem. Rev.* **2002**, *227*, 175-192. (h) Mathey, F.; Tran Huy, N. H.; Marinetti, A. Electrophilic Terminal-Phosphinidene Complexes: Versatile Phosphorus Analogues of Singlet Carbenes. *Helv. Chim. Acta* **2001**, *84*, 2938-2957. (i) Stephan, D. W. Zirconium-Phosphorus Chemistry: Strategies in Syntheses, Reactivity, Catalysis, and Utility. *Angew. Chem. Int. Ed.* **2000**, *39*, 314-329. (j) Shah, S.; Protasiewicz, J. D. 'Phospha-variations' on the themes of Staudinger and Wittig: phosphorus analogs of Wittig reagents. *Coord. Chem. Rev.* **2000**, *210*, 181-201.

3. García, M. E.; García-Vivó, D.; Ramos, A.; Ruiz, M. A. Phosphinidene-bridged binuclear complexes. *Coord. Chem. Rev.* **2017**, *330*, 1-36.
4. Graham, T. W.; Udachin, K. A.; Carty, A. J. Reactivity of electrophilic μ-phosphinidene complexes with heterocumulenes: formation of the first σ-π-aminophosphaimine complexes $[Mn_2(CO)_8\{\mu\text{-}\eta^1,\eta^2\text{-}P(N^iPr_2)=NR\}]$ and diazoalkane insertions into metal-phosphorus bonds. *Chem. Commun.* **2005**, 4441-4443.
5. Seidl, M.; Stubenhofer, M.; Timoshkin, A. Y.; Scheer, M. Reaction of Pentelidene Complexes with Diazoalkanes: Stabilization of Parent 2,3-Dipnictabutadienes *Angew. Chem. Int. Ed.* **2016**, *55*, 14037-14040.
6. Seidl, M.; Kuntz, C.; Bodensteiner, M.; Timoshkin, A. Y.; Scheer, M. Reaction of Tungsten–Phosphinidene and –Arsinidene Complexes with Carbodiimides and Alkyl Azides: A Straightforward Way to Four-Membered Heterocycles. *Angew. Chem. Int. Ed.* **2015**, *54*, 2771-2775.
7. Albuerne, I. G.; Alvarez, M. A.; Amor, I.; García, M. E.; García-Vivó, D.; Ruiz, M. A. Cycloaddition Reactions of the Phosphinidene-Bridged Complex $[Mo_2Cp(\mu\text{-}\kappa^1:\kappa^1,\eta^5\text{-}PC_5H_4)(CO)_2(\eta^6\text{-}HMes^*)]$ with Diazoalkanes and other Heterocumulenes. *Inorg. Chem.* **2016**, *55*, 10680-10691.
8. Alvarez, M. A.; García, M. E.; González, R.; Ruiz, M. A. Nucleophilic and Electrophilic Behavior of the Phosphinidene-Bridged Complex $[Fe_2(\eta^5\text{-}C_5H_5)_2(\mu\text{-}PCy)(\mu\text{-}CO)(CO)_2]$. *Organometallics* **2008**, *27*, 1037-1040.
9. Alvarez, M. A.; García, M. E.; González, R.; Ruiz, M. A. Reactions of the Phosphinidene-Bridged Complexes $[Fe_2(\eta^5\text{-}C_5H_5)_2(\mu\text{-}PR)(\mu\text{-}CO)(CO)_2]$ (R = Cy, Ph) with Electrophiles Based on p-Block Elements. *Dalton Trans.* **2012**, *417*, 14498-14513.

10. Alvarez, M. A.; García, M. E.; González, R.; Ruiz, M. A. Reactions of the Phosphinidene-Bridged Complexes $[Fe_2(\eta^5\text{-}C_5H_5)_2(\mu\text{-}PR)(\mu\text{-}CO)(CO)_2]$ (R = Cy, Ph, 2,4,6-$C_6H_2{}^tBu_3$) with Diazoalkanes. Formation and Rearrangements of Phosphadiazadiene-Bridged Derivatives. *Organometallics* **2010**, *29*, 5140-5153.
11. Albuerne, I. G.; Alvarez, M. A.; García, M. E.; García-Vivó, D.; Ruiz, M. A. Novel Dimerization of Maleic Anhydride at a $Mo_2$ Complex: Phase-Driven Keto/Enol Tautomerism in a Phosphinidenium-Ylide Complex. *Organometallics* **2013**, *32*, 6178-6181.
12. Albuerne, I. G.; Alvarez, M. A.; García, M. E.; García-Vivó, D.; Ruiz, M. A. Electronic Structure and Multisite Basicity of the Pyramidal Phosphinidene-Bridged Dimolybdenum Complex $[Mo_2(\eta^5\text{-}C_5H_5)(\mu\text{-}\kappa^1\text{:}\kappa^1,\eta^5\text{-}PC_5H_4)(\eta^6\text{-}C_6H_3{}^tBu_3)(CO)_2(PMe_3)]$. *Inorg. Chem.* **2015**, *54*, 9810-9820.
13. Albuerne, I. G.; Alvarez, M. A.; García, M. E.; García-Vivó, D.; Ruiz, M. A. Chemistry of $CS_2$- and SCNPh-adducts of the Pyramidal Phosphinidene-Bridged Dimolybdenum Complex $[Mo_2(\eta^5\text{-}C_5H_5)(\mu\text{-}\kappa^1\text{:}\kappa^1,\eta^5\text{-}PC_5H_4)(CO)_2(\eta^6\text{-}HMes^*)(PMe_3)]$. *Dalton Trans.* **2017**, *46*, 3510-3525.
14. Alvarez, B.; Alvarez, M. A.; Amor, I.; García, M. E.; García-Vivó, D.; Ruiz, M. A.; Suárez, J. Dimolybdenum Cyclopentadienyl Complexes with Bridging Chalcogenophosphinidene Ligands. *Inorg. Chem.* **2012**, *51*, 7810-7824.
15. Alvarez, M. A.; Amor, I.; García, M. E.; García-Vivó, D.; Ruiz, M. A.; Suárez, J. Reactivity of the Phosphinidene-Bridged Complexes $[Mo_2Cp(\mu\text{-}\kappa^1\text{:}\kappa^1,\eta^5\text{-}PC_5H_4)(\eta^6\text{-}1,3,5\text{-}C_6H_3{}^tBu_3)(CO)_2]$ and $[Mo_2Cp_2(\mu\text{-}PH)(\eta^6\text{-}1,3,5\text{-}C_6H_3{}^tBu_3)(CO)_2]$ Toward Alkynes: Multicomponent Reactions in the Presence of Ligands. *Organometallics* **2012**, *31*, 2749-2763.
16. (a) Alvarez, M. A.; Amor, I.; García, M. E.; García-Vivó, D.; Ruiz, M. A. Carbene- and Carbyne-like Behavior of the Mo–P Multiple Bond in a Dimolybdenum Complex Inducing Trigonal Pyramidal Coordination of a Phosphinidene Ligand. *Inorg. Chem.* **2007**, *46*, 6230-6232. (b) Alvarez, M. A.; Amor, I.; García, M. E.; García-Vivó, D.; Ruiz, M. A.; Suárez, J. Structure, Bonding and Reactivity of Binuclear Complexes having Asymmetric Trigonal Phosphinidene Bridges: Addition of 16-electron Metal Carbonyl Fragments to the Dimolybdenum Compounds $[Mo_2Cp(\mu\text{-}\kappa^1\text{:}\kappa^1,\eta^5\text{-}PC_5H_4)(CO)_2L]$ and $[Mo_2Cp_2(\mu\text{-}PH)(CO)_2L]$ (L = $\eta^6$-1,3,5-$C_6H_3{}^tBu_3$). *Organometallics* **2010**, *29*, 4384-4395.
17. Cordero, B.; Gómez, V.; Platero-Prats, A. E.; Revés, M.; Echevarría, J.; Cremades, E.; Barragán, F.; Alvarez, S. Covalent Radii Revisited. *Dalton Trans.* **2008**, 2832-2838.
18. Pyykkö, P.; Atsumi, M. Molecular Double-Bond Covalent Radii for Elements Li-E112. *Chem. Eur. J.* **2009**, *15*, 12770-12779.

19. Braterman, P. S. *Metal Carbonyl Spectra*; Academic Press: London, U. K., 1975.
20. Two-bond couplings involving P atoms ($^{2}J_{PX}$) in metal complexes increase algebraically with P–M–X angle, and therefore are quite sensitive to the relative positioning of P and X. Their absolute values for piano-stool complexes of type $MCpPXL_2$ usually follow the order $|^{2}J_{cis}| > |^{2}J_{trans}|$. See, for instance, Jameson, C. J. in *Phosphorus-31 NMR Spectroscopy in Stereochemical Analysis*; Verkade, J. G., Quin, L. D., Eds.; VCH: Deerfield Beach, FL, 1987; Chapter 6, and Wrackmeyer, B.; Alt, H. G.; Maisel, H. E. Ein- und zwei-dimensionale Multikern NMR-Spektroskopie an den isomeren Halbsandwich-Komplexen *cis*- und *trans*-[($\eta^5$-$C_5H_5$)W(CO)$_2$(H)PMe$_3$]. *J. Organomet. Chem.* **1990**, *399*, 125-130.
21. Bebbington, M. W. P.; Bourissou, D. Stabilised phosphazides. *Coord. Chem. Rev.* **2009**, *253*, 1248-1261.
22. (a) Staudinger, H.; Meyer, J. Über neue organische Phosphorverbindungen III. Phosphinmethylenderivate und Phosphinimine. *Helv. Chim. Acta.* **1919**, *2*, 635-646. (b) Gololobov, Y. G.; Kasukhin, L. F. Recent advances in the Staudinger reaction. *Tetrahedron* **1992**, *48*, 1353-1406. (c) Gololobov, Y. G. Years of Staudinger reaction. *Tetrahedron* **1981**, *37*, 437-472.
23. A search on the Cambridge Crystallographic Data Centre database yielded 10 compounds, with distances along the P–N–N–N chain in the ranges 1.64-1.67/1.30-1.35/1.26-1.31 Å respectively. For some examples see: (a) Fortman, G. C.; Captain, B.; Hoff, C. D. Thermodynamic Investigations of the Staudinger Reaction of Trialkylphosphines with 1-Adamantyl Azide and the Isolation of an Unusual s-cis Phosphazide. *Inorg. Chem.* **2009**, *48*, 1808-1810. (b) Meguro, T.; Yoshida, S.; Igawa, K.; Tomooka, K.; Hosoya, T. Transient Protection of Organic Azides from Click Reactions with Alkynes by Phosphazide Formation. *Org. Lett.* **2018**, *20*, 4126-4130.
24. (a) Creswick, M. W.; Bernal, I. The absolute configurations of organometallic compounds. XX. The conformations and absolute configurations of four preferred and non-preferred diastereoisomers having composition (R″-$C_5H_4$)Mo(CO)$_2$[(HCPhR)-N(CPh)-N(HCPhR′)] *Inorg. Chim. Acta* **1983**, *74*, 241-269. (b) Draux, M.; Bernal, I. The conformations and absolute configurations of two preferred diastereoisomers having composition ($CH_3C_5H_4$)Mo(CO)$_2$ [(HCPhR)N-C(Ph)-N(HCPhR′)]. *Inorg. Chim. Acta* **1986**, *114*, 75-86. (c) Fontaine, P. P.; Yonke, B. L.; Zavalij, P. Y.; Sita, L. R. Dinitrogen Complexation and Extent of N≡N Activation within the Group 6 "End-On-Bridged" Dinuclear Complexes, {($\eta^5$-$C_5Me_5$)M[N(i-Pr)C(Me)N(i-Pr)]}$_2$($\mu$-$\eta^1$:$\eta^1$-$N_2$) (M = Mo and W). *J. Am. Chem. Soc.* **2010**, *132*, 12273-12285.

25. Carty, A. J.; MacLaughlin, S. A.; Nucciarone, D. in *Phosphorus-31 NMR Spectroscopy in Stereochemical Analysis*; Verkade, J. G., Quin, L. D., Eds.; VCH: Deerfield Beach, FL, 1987; Chapter 16.
26. Garrou, P. $\Delta_R$ Ring Contributions to $^{31}$P NMR Parameters of Transition-Metal-Phosphorus Chelate Complexes. *Chem. Rev.* **1981**, *81*, 229-266.
27. (a) Cramer, C. J. *Essentials of Computational Chemistry, 2nd Ed.*; Wiley: Chichester, UK, 2004. (b) Koch, W.; Holthausen, M. C. *A Chemist´s Guide to Density Functional Theory, 2nd Ed.*; Wiley-VCH: Weinheim, 2002.
28. For $R_3P$-$N_3R'$adducts (also known as phosphazides), theoretical calculations indicate that the relative stability of *cis* and *trans* isomers would depend on substituents, although only *cis* isomers have the right geometry to undergo P–N bond formation with the remote NR´ group, to yield the cyclic intermediate preceding denitrogenation (see reference 21 and references therein). In our case, the possibility that the cisoid intermediates of type **B** (and not the transoid conformers **A**) are first formed in the reaction of compound **1** with azides is discarded because the lone pair in the remote NR´ atoms of conformers **B** point to an inner region of the molecule (see Figure 4 and SI). Such a conformation is well suited for intramolecular N–Mo or N–P bond formation, but not for nucleophilic attack on an external electrophile (MeI), so conformers of type **B** hardly could be precursors of compounds like **6**.
29. Alvarez, M. A.; García, M. E.; Ruiz, M. A.; Suárez, J. Enhanced Nucleophilic Behaviour of a Dimolybdenum Phosphinidene Complex: Multicomponent Reactions with Activated Alkenes and Alkynes in the Presence of CO or CNXyl. *Angew. Chem. Int. Ed.* **2011**, *50*, 6383-6387.
30. Armarego, W. L. F.; Chai, C. *Purification of Laboratory Chemicals*, *7th ed.*; Butterworth-Heinemann: Oxford, U. K., 2012.
31. Miller, J. B. Preparation of Crystalline Diphenyldiazomethane. *J. Org. Chem.* **1959**, *24*, 560-561.
32. Vogel, A. I. *Textbook of Practical Organic Chemistry, 4th ed.*; Longmans: London, U. K., 1978, p 291.
33. Yakelis, N. A.; Bergman, R. G. Safe Preparation and Purification of Sodium Tetrakis[(3,5-trifluoromethyl)phenyl]borate ($NaBArF_{24}$): Reliable and Sensitive Analysis of Water in Solutions of Fluorinated Tetraarylborates. *Organometallics* **2005**, *24*, 3579-3581.
34. (*a*) Nishida, H.; Takada, N.; Yoshimura, M.; Sonoda T.; Kobayashi, H. Tetrakis[3,5-bis(trifluoromethyl)phenyl]borate. Highly Lipophilic Stable Anionic Agent for Solvent-extraction of Cations. *Bull. Chem. Soc. Jpn.* **1984**, *57*, 2600-2604. (*b*) Brookhart, M.; Grant B.; Volpe Jr., A. F. [(3,5-

$(CF_3)_2C_6H_3)_4B]^-[H(OEt_2)_2]^+$: a convenient reagent for generation and stabilization of cationic, highly electrophilic organometallic complexes. *Organometallics* **1992**, *11*, 3920-3922.

35. *CrysAlis Pro*; Oxford Diffraction Limited, Ltd.: Oxford, U. K., 2006.
36. Farrugia, L. J. WinGX suite for small-molecule single-crystal crystallography. *J. Appl. Crystallogr.* **1999**, *32*, 837-838.
37. (a) Sheldrick, G. M. A short history of SHELX. *Acta Crystallogr., Sect. A* **2008**, *64*, 112-122. (b) Sheldrick, G. M. Crystal structure refinement with SHELXL. *Acta Crystallogr., Sect. C* **2015**, *71*, 5-8.
38. Spek, A. L. PLATON SQUEEZE: a tool for the calculation of the disordered solvent contribution to the calculated structure factors. *Acta Crystallogr. Sect. C* **2015,** *71*, 9-18.
39. Spek, A. L. *PLATON, A Multipurpose Crystallographic Tool*. Utrecht University: Utrecht: The Netherlands, 2010.
40. *APEX 2, version 2.0-1*, Bruker AXS Inc: Madison, WI, 2005.
41. *SMART & SAINT Software Reference Manuals, Version 5.051*; Bruker AXS Inc: Madison WI, 1998.
42. Sheldrick, G. M. *SADABS, Program for Empirical Absorption Correction*; University of Göttingen: Göttingen, Germany, 1996.
43. Frisch, M. J.; Trucks, G. W.; Schlegel, H. B.; Scuseria, G. E.; Robb, M. A.; Cheeseman, J. R.; Scalmani, G.; Barone, V.; Mennucci, B.; Petersson, G. A.; Nakatsuji, H.; Caricato, M.; Li, X.; Hratchian, H. P.; Izmaylov, A. F.; Bloino, J.; Zheng, G.; Sonnenberg, J. L.; Hada, M.; Ehara, M.; Toyota, K.; Fukuda, R.; Hasegawa, J.; Ishida, M.; Nakajima, T.; Honda, Y.; Kitao, O.; Nakai, H.; Vreven, T.; Montgomery, J. A., Jr.; Peralta, J. E.; Ogliaro, F.; Bearpark, M.; Heyd, J. J.; Brothers, E.; Kudin, K. N.; Staroverov, V. N.; Kobayashi, R.; Normand, J.; Raghavachari, K.; Rendell, A.; Burant, J. C.; Iyengar, S. S.; Tomasi, J.; Cossi, M.; Rega, N.; Millam, J. M.; Klene, M.; Knox, J. E.; Cross, J. B.; Bakken, V.; Adamo, C.; Jaramillo, J.; Gomperts, R.; Stratmann, R. E.; Yazyev, O.; Austin, A. J.; Cammi, R.; Pomelli, C.; Ochterski, J. W.; Martin, R. L.; Morokuma, K.; Zakrzewski, V. G.; Voth, G. A.; Salvador, P.; Dannenberg, J. J.; Dapprich, S.; Daniels, A. D.; Farkas, Ö.; Foresman, J. B.; Ortiz, J. V.; Cioslowski, J.; Fox, D. J. ; *Gaussian 09, Revision A.02*; Gaussian, Inc.: Wallingford, CT, USA, 2009.
44. Zhao Y.; Truhlar, D. G. A new local density functional for main-group thermochemistry, transition metal bonding, thermochemical kinetics, and noncovalent interactions. *J. Chem. Phys.* **2006**, *125*, 194101: 1-18.

45. Hay, P. J.; Wadt, W. R. Ab initio effective core potentials for molecular calculations. Potentials for potassium to gold including the outermost core orbitals. *J. Chem. Phys.* **1985**, *82*, 299-310.

46. (a) Hariharan, P. C.; Pople, J. A. Influence of polarization functions on MO hydrogenation energies. *Theor. Chim. Acta* **1973**, *28*, 213-222. (b) Petersson, G. A.; Al-Laham, M. A. A complete basis set model chemistry. II. Open-shell systems and the total energies of the first-row atoms. *J. Chem. Phys.* **1991**, *94*, 6081-6090. (c) Petersson, G. A.; Bennett, A.; Tensfeldt, T. G.; Al-Laham, M. A.; Shirley, W. A.; Mantzaris, J. A complete basis set model chemistry. I. The total energies of closed-shell atoms and hydrides of the first-row elements. *J. Chem. Phys.* **1988**, *89*, 2193-2218.

## (For Table of Contents Use Only)

### Table of Contents Synopsis

Reactions of compound **1** with diazoalkanes and organic azides proceed with P–N bond formation at the terminal atom of the organic reagent to yield unstable *P*:*P*-bridged phosphadiazadiene- and phosphatriazadiene derivatives, which can be stabilized through protonation or methylation reactions. The neutral phosphatriazadiene complexes may undergo competitive decarbonylation and N–Mo bond formation processes to yield phosphametallacyclic derivatives, instead of the most favored denitrogenation leading to phosphaimine derivatives.

### Graphics for Table of Contents